UNIVERSIDADE DE LISBOA
FACULDADE DE CIÊNCIAS
DEPARTAMENTO DE FÍSICA

High-throughput automatized reach-to-grasp setup to study motor control and movement patterns

Afonso Manuel Saraiva Germano

Mestrado em Engenharia Biomédica e Biofísica

Dissertação orientada por:
Prof. Dr. Nuno Miguel de Pinto Lobo e Matela
Prof. Dr. Joaquim Alves da Silva

2025

"I would rather have questions that can't be answered than answers that can't be questioned."

— Richard Feynman

Acknowledgements

This dissertation marks the conclusion of 5 years of work and, above all, a journey of learning and personal growth, the last step in my personal Engineering 101, where curiosity, late nights and a little duct tape solved more problems than I ever expected.

I would like to begin by thanking Joaquim, who taught me so much, not only about science but also about how to face challenges. Thank you for showing me the value of failing fast, for encouraging me to be proactive, and for instilling the importance of doing things with care and precision. Your guidance and rigour have been fundamental to my development as a person.

To Professor Matela, I extend my deepest gratitude. Over the past five years, you have consistently stood out for the way you teach, understand and communicate with your students. I was fortunate to be one of them. Your dedication and passion for education are truly inspiring, and I am grateful for every lesson you have shared.

Within the Champalimaud Foundation, I am thankful to everyone who welcomed me from the very beginning, shared their knowledge and ideas, and offered help even when it was far beyond their responsibilities. More than scientific skills, I learned a great deal about life itself during spontaneous conversations that I will always remember.

A special thank you goes to my lab, the teaching lab and all the support platforms, especially the hardware and software teams. I am grateful to everyone who accompanied me to the vivarium to handle the mice, to those who helped me code, tighten a screw or design something in 3D. Each gesture, each explanation and every word of encouragement made a difference. To all who challenged me, inspired me and sparked new curiosities, I am profoundly grateful.

To my friends throughout these university years, thank you for every shared moment, for the beers, the housemates, the travels, the late-night projects and, most of all, for growing alongside me. Each of you, without exception, has helped me become a better person.

To my oldest friends, thank you for the endless laughter on nights out, the late gaming sessions and the long lunches that always helped me unwind and reset.

Finally, to my family, my greatest foundation. To my Mom and Dad, whose care and strenght have carried me through every challenge, often feeling my nerves more than I did before presentations or when things did not go as planned. To Vanessa, Paulo, Laura and Júlia, the people with whom I have spent most of my time in recent years, thank you for welcoming me, supporting me and making me feel special. Your love, encouragement and unwavering belief in me have been a constant source of comfort and courage, reminding me of what truly matters.

Abstract

Research on skilled motor control in rodents often faces significant limitations, including low trial throughput, heavy reliance on manual supervision, and limited ecological validity. This work addresses these challenges through the design and validation of a high-throughput, automated system for measuring skilled forelimb movements in mice. The platform was engineered to operate continuously in a home-cage environment while preserving experimental rigour and animal welfare, thereby enabling long-term, minimally supervised behavioural studies.

The reach-to-grasp task was chosen as the benchmark behaviour because it reliably evokes precise and repeatable forelimb movements, providing a stringent test of hardware and analytical performance. A custom reaching chamber was developed and progressively refined to automate water delivery, video capture, and data logging. Infra-red illumination and a single high-speed camera, combined with a 45° mirror, ensured stable, high-resolution recordings suitable for kinematic analysis. The resulting motion-tracking pipeline, based on DeepLabCut, accurately extracted trajectories and derived metrics such as velocity, acceleration, and movement smoothness.

To extend the task to a 24/7 setting, the chamber was integrated with the home-cage through a door mechanism featuring radio frequency identification (RFID) and a passive stopper system. This solution guarantees reliable individualisation and prevents multiple entries without introducing stress, highlighting the importance of aligning engineering design with natural behaviour.

Pilot experiments confirmed the system's stability and compatibility with parallel physiological recordings, including electromyography and *in vivo* calcium imaging. Although task-specific dystonia served as a proof-of-concept application, the platform itself is disease-agnostic. Its modular architecture, automated control, and scalable data acquisition provide a robust foundation for longitudinal studies of motor learning, adaptation, and pathology, bridging the gap between tightly controlled laboratory tasks and naturalistic behaviour.

Keywords: high-throughput behaviour, motion tracking, motor control, reach-to-grasp, task-specific dystonia

Resumo

O estudo do controlo motor em roedores enfrenta, há décadas, um conjunto de limitações que dificultam a obtenção de dados comportamentais ricos e com elevada validade ecológica. Tradicionalmente, a maioria dos paradigmas baseia-se em sessões de curta duração, com um único animal e forte dependência de intervenção manual. Este modelo não só reduz o número de sessões possíveis por unidade de tempo, como também limita a realização de experiências prolongadas capazes de revelar alterações progressivas do comportamento motor. Além disso, a frequente presença humana durante as experiências tende a criar condições que se afastam do contexto natural dos animais, podendo introduzir fatores de stress e/ou influenciar o comportamento dos animais.

A presente dissertação teve como objetivo ultrapassar estas barreiras através do desenvolvimento de uma plataforma automatizada, de elevado rendimento, para a medição de movimentos finos do membro anterior em ratinhos. O propósito central não foi estudar uma doença específica, mas sim criar uma ferramenta flexível, capaz de sustentar estudos longitudinais de aprendizagem e adaptação motora, com a mínima necessidade de supervisão humana. Ao disponibilizar um sistema que combina rigor experimental, escalabilidade e validade ecológica, esta plataforma pretende servir de base para futuras investigações em neurociência comportamental e translacional.

Para testar e validar o sistema, escolheu-se o paradigma *reach-to-grasp*, uma tarefa comportamental clássica que exige aos animais movimentos hábeis e precisos do membro anterior para obter uma recompensa. Este paradigma é amplamente utilizado em estudos de controlo motor por permitir a recolha de movimentos repetitivos e altamente padronizados, servindo assim como modelo de referência para o desenvolvimento e validação do hardware e do software, permitindo avaliar de forma eficaz a capacidade do sistema em registar e analisar ações motoras complexas.

A primeira fase do trabalho concentrou-se na construção de uma câmara de *reaching* totalmente personalizada, feita em acrílico, onde o animal se situava para realizar a tarefa. O desenho baseou-se em conceitos de estudos anteriores, mas foi adaptado para satisfazer as exigências específicas do projeto. Foi criada uma ranhura frontal que obriga à extensão completa da pata, permitindo controlar qual o membro utilizado através da posição lateral da água. O fornecimento de água é feito em gotas de volume definido, possibilitando ajustar a dificuldade do treino e garantir motivação adequada através de um regime controlado de restrição. Toda a estrutura foi montada numa *breadboard* modular, assegurando alinhamento rigoroso e facilidade de desmontagem para limpeza.

Um dos aspetos cruciais para a fiabilidade do sistema é a consistência das condições de iluminação e de posicionamento dos componentes, uma vez que pequenas variações podem comprometer a análise de imagem. Para contornar este problema recorreu-se a iluminação por infravermelhos e a um único sistema ótico, em que uma câmara de alta velocidade capta a imagem lateral e um espelho a 45° fornece a vista frontal. Esta solução, mais económica do que utilizar duas câmaras, revelou-se suficiente para uma reconstrução cinemática de elevada resolução.

A captura de vídeo, a entrega de gotas de água e o registo de dados foram totalmente automatizados

através de *software* desenvolvido em *Bonsai RX*. Em vez de gravar continuamente, o sistema deteta eventos de *reaching* e guarda apenas pequenos *clips* correspondentes a cada tentativa, otimizando o armazenamento e reduzindo a intervenção humana ao máximo.

Com os vídeos obtidos, foi implementado um *pipeline* de análise de movimento baseado em *DeepLabCut* que permite rastrear pontos anatómicos do membro anterior e extrair métricas como trajetória, velocidade, aceleração e suavidade do movimento. Esta abordagem confirmou a elevada qualidade das gravações e demonstrou a robustez do sistema para captar características motoras subtis. Em experiências de teste, observou-se por exemplo que ratinhos *wild-type* apresentaram uma tendência para diminuir o erro de direção inicial ao longo do tempo, enquanto animais portadores da mutação DYT-TOR1A permaneceram estáveis. Embora estes resultados sejam preliminares, ilustram a capacidade do sistema para detetar diferenças de aprendizagem motora e servir de base para futuros estudos.

Numa fase seguinte, a câmara de *reaching* foi integrada na *home-cage* dos ratinhos, permitindo que os animais executassem a tarefa de forma contínua, em regime 24 horas por dia, sem a presença humana. Esta etapa exigiu o desenvolvimento de uma porta que garantisse a identificação individual e prevenisse a entrada simultânea de vários ratinhos. Inicialmente testou-se uma porta rotativa acionada por um motor, tecnicamente avançada mas que gerava ruído e movimentos inesperados. Os animais reagiram com comportamentos de recuo, demonstrando que a solução ideal do ponto de vista da engenharia pode falhar quando não considera a perceção e o bem-estar do animal.

A solução final consistiu num sistema passivo com leitura RFID (radio frequency identification), em que cada animal é identificado ao aproximar-se e empurra livremente uma porta que funciona em conjunto com um *stopper* para impedir múltiplas entradas. Esta abordagem revelou-se silenciosa, previsível e compatível com o comportamento natural dos ratinhos, garantindo simultaneamente controlo experimental e redução do stress.

Outro avanço importante foi a verificação da compatibilidade do sistema individual com registos fisiológicos em paralelo, como eletromiografia e obtenção de imagens de cálcio *in vivo*, demonstrando que o sistema pode integrar medições neuronais ou musculares enquanto recolhe dados cinemáticos. Esta capacidade abre caminho a estudos multimodais que correlacionem atividade neuronal com parâmetros de movimento, ampliando o alcance translacional da ferramenta.

Embora o caso específico da distonia tenha sido usada como exemplo de aplicação, a plataforma é agnóstica em relação ao modelo de doença. A sua arquitetura modular permite adaptar facilmente o sistema a outros paradigmas comportamentais ou a diferentes objetivos de investigação, desde a aprendizagem motora básica até ao estudo de doenças do movimento. Entre as melhorias futuras sugeridas incluem-se a integração de sensores de peso ou pressão no mecanismo de entrada, calibrados à massa corporal dos ratinhos, para maior precisão no controlo de acesso, bem como a adição de sensores de bolhas no circuito de água para evitar falsas contagens.

Em termos de impacto, esta dissertação demonstra que é possível conciliar reprodutibilidade laboratorial com um contexto naturalístico, permitindo recolher grandes volumes de dados de forma automatizada e com mínima interferência. O sistema garante identificação individual fiável, opera de forma contínua e suporta experiências prolongadas que antes seriam logisticamente impraticáveis.

Além disso, a plataforma contribui para o bem-estar animal, uma vez que os ratinhos podem explorar livremente o ambiente, decidir quando realizar a tarefa e permanecer em grupo, reduzindo o stress associado a manipulações frequentes ou ao isolamento. O sistema de fornecimento de água é monitorizado e inclui mecanismos de reposição automática, garantindo que a motivação dos animais é mantida sem comprometer a hidratação.

Em síntese, esta dissertação apresenta um sistema de alta capacidade e automatização integral que

representa um avanço significativo na investigação do comportamento motor em roedores. A combinação de tecnologia de visão computacional, controlo automatizado e desenho modular cria uma ferramenta robusta, escalável e facilmente adaptável a múltiplos contextos experimentais. Ao possibilitar monitorização contínua, análises cinemáticas de alta resolução e integração com registos fisiológicos, a plataforma abre novas perspetivas para estudos que pretendam compreender os mecanismos do controlo motor, de aprendizagem e de disfunções associadas.

O trabalho aqui descrito demonstra que, ao alinhar soluções de engenharia com as necessidades e o comportamento natural dos animais, é possível criar infraestruturas experimentais de próxima geração, capazes de suportar tanto abordagens exploratórias como estudar hipóteses bem definidas. Desta forma, esta plataforma estabelece as bases para futuras investigações em neurociência translacional, fornecendo um recurso versátil para a comunidade científica que procura compreender, de forma detalhada, a dinâmica do movimento e da adaptação motora ao longo do tempo.

Palavras chave: comportamento de alto rendimento, controlo motor, distonia de tarefa específica, *reach-to-grasp*, registo de movimento

Scientific output

M.V. Bettencourt, **A. Germano**, F. França de Barros J. Alves da Silva, "A High-Throughput 24/7 Reach-to-Grasp System for Investigating Motor Control and Movement Disorders", abstract submission and poster presentation at XIX Meeting of the Portuguese Society of Neuroscience, 28-30 May 2025, Póvoa de Varzim, Portugal (see Appendix A).

A. Germano, J. Alves da Silva, "A High-Throughput 24/7 Reach-to-Grasp System for Investigating Motor Control and Movement Disorders", abstract submission and oral presentation at IMED Innovate Competition 17.0, 3 October 2025, Lisbon, Portugal (see Appendix B).

Table of Contents

List of Figures

List of Tables

List of Acronyms

API average pixel intensity. 19, 20

DLC DeepLabCut. 7–9, 13, 22, 23, 35, 49

DYT DYT1 knock-in mutants. 25, 27–29, 36, 38–41, 49

DYT-TOR1A early onset torsion dystonia caused by a mutation in the TOR1A gene encoding the protein torsinA. 11, 48

EMG electromyography. 15, 28, 35, 39, 40

MSNs medium spiny neurons. 40, 41

MT motion tracking. 1, 7, 33

ORT one-rat turnstile. 10, 11

RFID radio frequency identification. vi, viii, 10, 11, 16–18, 20, 21, 29–31, 45, 47, 49

ROI region of interest. 19, 20

RtG reach-to-grasp. 1, 2, 5, 12–14, 16, 18, 21–23, 28, 36, 37, 39, 41, 46–49

SLEAP Social LEAP Estimates Animal Poses. 7

WT wild-type. 25, 27–29, 36, 38–41, 49

Chapter 1

Introduction

1.1 Contextualization and motivation

The observation of movement enables a direct and quantifiable way to study behaviour, as it provides a reflection of how organisms interact with their environment. Based on this principle, movement analysis has long been used as a window into both motor control and broader behavioural processes. What began with basic videography and manual scoring [1] has progressively evolved into a technologically-driven field, in which engineering solutions play a central role.

Recent advances in motion tracking (MT) techniques, computer vision, and machine learning have transformed how behavioural neuroscience can be conducted [2], [3], [4], [5]. These developments allow for the quantification of behaviours that were once regarded as qualitative, refining both the precision of data collection and the reliability of analysis. From full-body movements to fine motor actions, the integration of neuroengineering tools has enabled more robust and scalable approaches to studying behaviour.

In parallel, the use of animal models, particularly mice, has remained fundamental in uncovering the mechanisms underlying movement and its dysfunction [6], [7], [8]. Within this context, the reach-to-grasp (reach-to-grasp (RtG)) task has long been used as a valuable experimental paradigm. It captures goal-directed forelimb actions, similar to those observed in natural foraging and provides a structured framework to study voluntary dexterous movement [9], [10], [11]. However, the application of long-term RtG paradigms, especially those where a high-throughput is required, has been hindered. This is particularly due to the continued reliance on manual intervention of the experimenter and the limited throughput in many of the existing designs.

This dissertation is motivated by the need to address these limitations using automation and engineering optimisation. The central objective is to design and validate an automated, water-based RtG setup that ensures precise delivery, synchronisation, and recording of behavioural events while operating continuously with minimal human intervention. By embedding individualisation strategies and MT techniques, the here proposed setup aims to support longitudinal studies in group-housed mice, overcoming key bottlenecks in current approaches.

This project contributes to bridging the gap between behavioural neuroscience and engineering innovation, increasing the efficiency of motor control research with a novel system that enables high-throughput long-term paradigms.

1.2 Objectives

The main goal of this dissertation is to develop a high-throughput, automatised RtG setup to investigate motor control and movement patterns. This setup will be later employed in motor control experiments with the goal of studying movement disorders, namely, dystonia. Thus, this project aims to contribute to the field of motor control by providing a robust and versatile platform to analyse movement dynamics in a continuous and autonomous manner. To achieve this goal, three key aims were formulated:

1. Design and construct a reaching chamber optimised for water-based operant conditioning tasks, that ensures precise delivery, recording, and synchronisation of behavioural events.
2. Develop and implement a motion tracking pipeline that enables accurate kinematic analysis of forelimb movement.
3. Adapt the setup for longitudinal operation, creating a neuroethological context for the mice and minimizing the need for human intervention while ensuring reliable data collection over extended periods.

By achieving these objectives, this dissertation seeks to contribute a novel and high-impact tool for motor control research, with applications ranging from basic science to clinical research. While this setup will be applied here in the context of movement disorders and task-specific dystonia, it is designed to be broadly generalisable, supporting its use for testing numerous hypotheses in diverse scientific fields.

1.3 Structure

This dissertation is organised into seven chapters. Chapter 1 introduces the dissertation theme, providing its context, motivation, aims, and structure. Chapter 2 presents the theoretical background and state-of-the-art relevant to the investigation. Chapter 3 details the materials and methods, including the technological developments, the analysis pipeline, and the experimental procedures. Chapter 4 reports and discusses the results obtained from the experiments. Chapter 5 proposes a protocol, consolidating the guidelines required to replicate the study. Chapter 6 concludes the dissertation by summarising the main findings and offering perspectives for future research. Finally, Chapter 7 contains appendices and supplementary material.

Chapter 2

Background Theory

2.1 Neuroethological experiments

Neuroethological experiments aim to study behaviour in contexts that preserve key aspects of an animal's natural repertoire while still allowing scientific observation and measurement [12], [13]. This approach has been extensively explored and has led to methods that improve animal welfare, reduce stress, and provide richer, more ecologically valid datasets. By observing behaviours that emerge spontaneously in semi-naturalistic conditions, researchers can collect longitudinal data with minimal intervention while maintaining ethical standards.

Different species such as mice, rats, and primates may be used in these experiments [8]. This dissertation focuses on the development of a system that enables neuroethological experiments designed for mice. Mice offer distinct advantages for high-throughput and longitudinal studies due to their small size, rapid breeding cycle, and ease of handling [7]. Moreover, their nervous system shares fundamental organisational and functional similarities with that of humans, providing strong translational potential for modelling neurological disorders and testing therapeutic strategies [14], [15]. Additionally, the availability of a wide range of transgenic lines [16] further allows precise manipulation of specific genes and neural circuits, enabling the detailed investigation of targeted behavioural and neurobiological mechanisms.

The continuous advancement of neuroethological approaches is made possible through the development of science namely, engineering. Technological innovation provides the tools to design systems that combine naturalistic environments with precise control, enabling sophisticated, automated, and scalable observation. This synergy between neuroscience and engineering allows researchers to study behaviour in increasingly rich and complex settings while maintaining rigorous scientific standards. Such paradigms and technological advances are useful across multiple domains of neuroscience and, in the context of this work, provide a framework that can be applied to the study of motor behaviour, laying the foundation for the next generation of experimental setups.

2.2 Task-based experiments

Motor control studies often rely on structured paradigms that allow for the isolation and quantification of specific movement parameters. Task-based models serve this purpose by providing controlled environments in which animals are required to perform defined actions, enabling the measurement of various variables.

These models have evolved alongside technological progress, incorporating automatization, real-time tracking, and precise stimulus delivery. Such integration has improved throughput, reduced observer bias, and increased the reproducibility of behavioural assays.

Examples include lever-press paradigms and reaching tasks, which will be further detailed in the following subsections.

2.2.1 Lever press

Lever press paradigms are commonly used to study motivated behaviour and basic motor skills. Animals learn to perform goal-directed actions like pressing a lever in exchange for a reward, typically under scheduled reinforcement [17]. In this context, scheduled reinforcement refers to the rule governing how and when a reward is delivered after a lever press. For instance, reinforcement can be provided every time the lever is pressed, after a set number of presses, after varying numbers of presses or according to specific time intervals [17]. These schedules strongly influence the rate, persistence, and pattern of responding, allowing researchers to probe motivation, learning strategies, and motor output under different contingencies.

Over time, this approach has evolved considerably, particularly through its integration into operant conditioning chambers (Skinner boxes) [18], [19]. These systems have become increasingly modular and technologically advanced, incorporating various plug-ins that expand experimental flexibility and precision, as seen in Figure 2.1. Examples include lick-o-meters to monitor consummatory behaviour [20], speakers to deliver auditory cues [21], and electrified grids for aversive conditioning [22]. These additions allow researchers to manipulate and monitor multiple sensory modalities and motivational contexts, enabling more refined analysis of learning, decision-making, and motor output.

While the lever press task remains relatively simple in terms of motor demands, modifications to reinforcement schedules, stimulus types, or task structure can significantly influence the behavioural strategies adopted by the animals. This makes the paradigm valuable not only for high-throughput behavioural assessment, but also for exploring how animals adapt their motor responses under varying cognitive and environmental constraints. [23], [24]. However, because lever pressing does not require dexterous motor control, it was not considered suitable for our study.

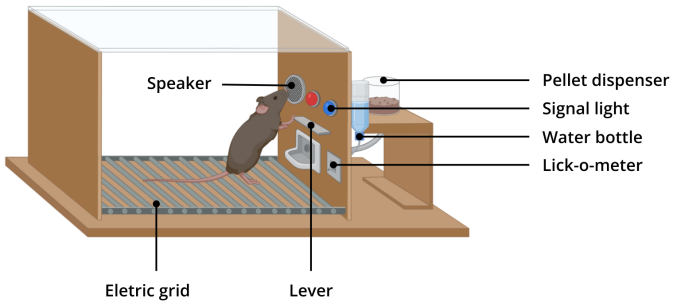

Figure 2.1: Schematic representation of the Skinner Box, which includes the lever press task; created with BioRender.com.

2.2.2 Reach-to-grasp

The RtG task involves coordinated movements of the upper limbs and requires precise control of both motion and grip. It is designed to probe skilled forelimb use by requiring animals to reach for and retrieve various objects, such as food pellets or water droplets [10], [25]. Given the conserved motor patterns and neural mechanisms across species [6], rodent reach-to-grasp models provide a relevant framework and are particularly valuable for studying kinematics, offering insights into trajectory planning, grip strategy, and movement efficiency [25], [26], [27].

Although single-pellet tasks remain widely used and are considered the standard for assessing forelimb motor function in rodents, they potentially face several limitations, such as a low number of repetitions per session due to the relatively large reward size and, in the case of electrophysiological recordings, possible artefacts provoked by jaw movements during pellet chewing [28], [29], [30].

In contrast, water-based reach-to-grasp tasks have emerged as a compelling alternative to pellet-based approaches, providing strong motivational properties, ease of precise and automated delivery, and the absence of chewing artefacts [10]. Although they may not demand the same level of dexterity as pellet retrieval, these tasks still require fine forelimb control, making them a suitable paradigm for investigating skilled motor behaviour.

Depending on the experimental goals, this task can be performed in head-fixed or freely moving conditions. For the purpose of high-resolution neural recordings, head-fixed configurations provide superior experimental control, as the animal is in a restricted and more easily standardised environment [27]. Nevertheless, freely moving configurations offer a more naturalistic context that still allows for the dissection of motor behaviour [31], [32], but also introduce technical challenges such as unrestricted movement, which require tailored engineering solutions for precise tracking and behavioural quantification.

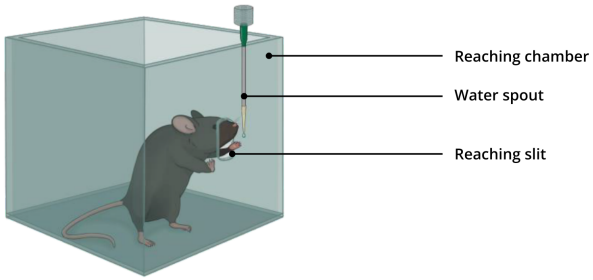

Figure 2.2: Schematic representation of the reach-to-grasp task.

Despite these advances, most reach-to-grasp paradigms remain constrained by short, individual sessions, limiting the number of repetitions and longitudinal assessment.

2.3 Methodologies in high-throughput behavioural research

Given the complexity of behavioural experiments, careful design of both data collection and analysis is essential to support automatisation, reproducibility, and scalability. By establishing structured and consistent methodologies, researchers can minimise variability, reduce human bias, and enable the integration of advanced computational approaches. In this section, we provide an overview of the current state-of-the-art methods for data acquisition, analysis, and concrete examples of high-throughput experimental setups.

2.3.1 Recording animal behaviour

The collection of behavioural data can take place in a wide range of contexts, from natural habitats to highly controlled laboratory environments. While field studies provide ecological validity and allow the observation of spontaneous behaviours in dynamic settings, laboratory experiments offer a level of control that is critical for identifying causal relationships and isolating specific variables. For neuroscience and behavioural studies, where subtle motor patterns or stimulus-response dynamics are often investigated, such control is essential for ensuring experimental rigour and reproducibility.

In practice, neuroscience experiments frequently rely on the simultaneous use of multiple techniques. For example, an experiment designed to optically measure neural activity in a specific brain area while the animal moves freely in an open field would require a camera to track locomotion and a separate system to record the neural signals. Typically, each of these techniques comes with its own dedicated software, which complicates their integration. In such scenarios, there is a clear need for tools that unify data streams, synchronise devices, and facilitate real-time coordination of experimental events.

A widely used tool in this context is Bonsai RX, an open-source visual programming language designed for real-time control and data processing [33]. With its user-friendly interface, Bonsai RX enables the creation of real-time closed-loop systems, facilitating the construction of experimental pipelines.

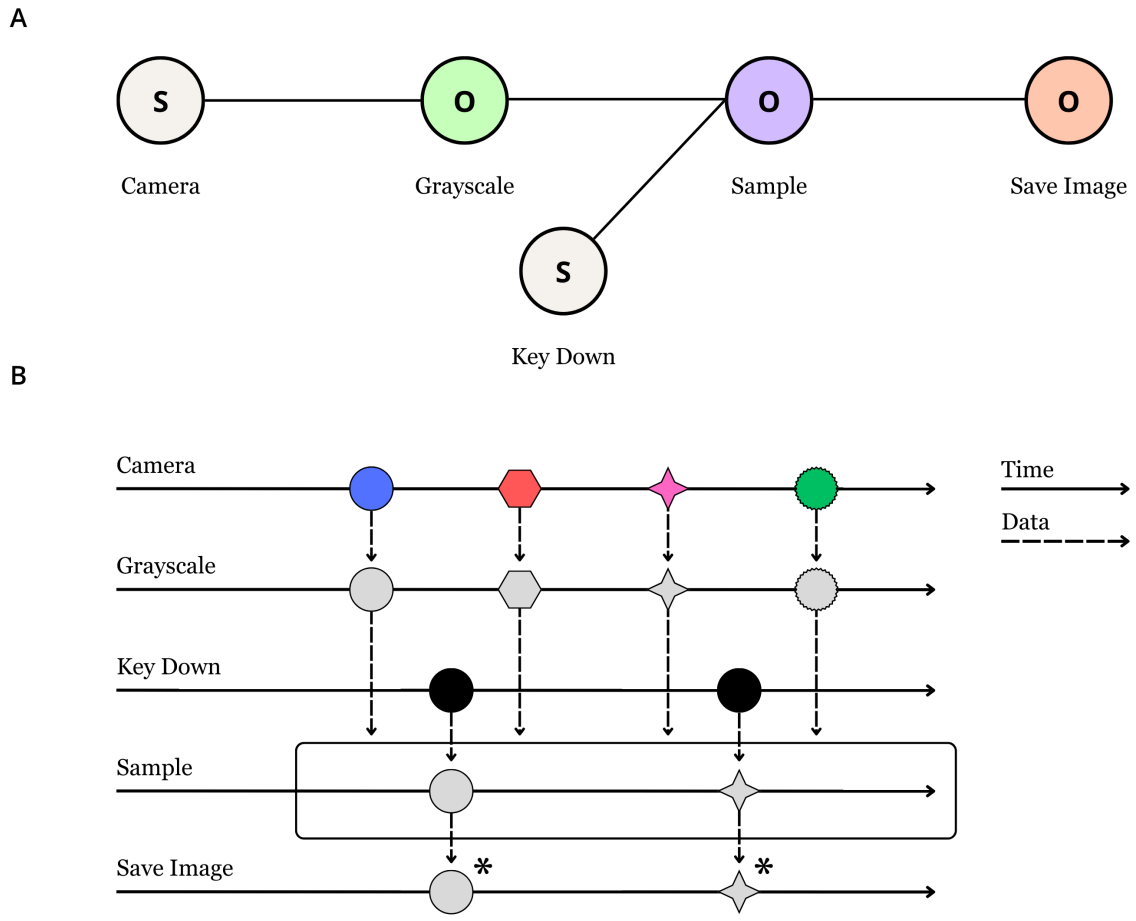

Figure 2.3: Example of Bonsai RX dataflow for capturing greyscale images upon key press. The top part (A) shows a visual representation of the dataflow, where circles marked "S" represent data sources (Camera and Key Down), while circles marked "O" represent operators (Greyscale, Sample, and Save Image). The flow shows how a camera stream is processed into greyscale, sampled upon keyboard events, and stored as images. The bottom part (B) shows a marble diagram representing the temporal behaviour of this flow, where coloured tokens represent frames emitted by the camera, black dots indicate key press events, and asterisks represent image-saving operations triggered by those key events. Adapted from Lopes *etl al.* [33]

As illustrated in Figure 2.3, in Bonsai RX, data streams are handled as continuous observable sequences. These sequences are manipulated and processed through a dataflow representation, where nodes represent either data sources (*e.g.*, video or sensor inputs) or operators (elements that transform, filter, or act upon the data stream) [33]. This structure allows for flexible, real-time handling of behavioural data, supporting high-throughput experimental setups.

Within the context of MT, Bonsai RX provides several tools that can be used to improve and automate various stages of data acquisition and analysis. For example, it facilitates the implementation of event-based acquisition strategies, allowing selective and real-time data capture triggered by specific behavioural events. This approach not only enhances the efficiency of experiments but also reduces data storage demands by avoiding continuous recording. These automation features contribute to more streamlined workflows and will be further explored in Chapter 3.1.2.

Additionally, its modular design promotes best practices in code development by making workflows more maintainable and adaptable. This flexibility allows researchers to easily modify existing protocols or integrate new functionalities as experimental needs evolve, thereby supporting continuous improvement and innovation in data acquisition.

2.3.2 Analysing animal behaviour

Historically, behavioural and kinematic data were analysed manually, which made the process slow, labour-intensive and prone to errors. This approach has become highly inefficient due to the exponential growth in the speed and volume of data collection, which far exceeds the capacity of manual methods to process and analyse information in a timely and accurate manner [2], [34], [35], [36].

Here, we are especially interested in tracking the animal's pose, so that we can subsequently analyse their movements with greater precision, quantify behavioural patterns over time, and identify subtle motor deficits that would be difficult to detect through manual observation alone.

For this end, the gold standard has been shifting from the combination of video recordings and reflective markers applied to regions of interest, towards markerless motion tracking techniques that leverage deep learning algorithms to automatically identify and track body parts directly from raw video footage [2], [37], [38]. Current state-of-the-art methods, such as DeepLabCut (DLC) or Social LEAP Estimates Animal Poses (SLEAP), are deep learning-based approaches that rely on user-annotated training data and convolutional neural networks to accurately track the pose of single or multiple animals across frames, without the need for physical markers [2], [38], [39]. The key advantage of convolutional neural networks lies in their ability to learn hierarchical representations of visual features [40], allowing them to robustly recognise body parts under different poses, lighting conditions, and backgrounds. This capacity is precisely what has enabled the development of reliable and scalable markerless tracking methods suitable for complex behavioural analyses.

In this work, we focus specifically on DLC, which was selected for our pose estimation pipeline not only because of its robustness and prior adoption in our laboratory, but also due to its suitability for high-precision, single-animal tracking. While alternatives such as SLEAP have been developed primarily for multi-animal tracking and can handle single-animal scenarios, they are not optimised for capturing detailed, fine-grained kinematics within a single subject. In contrast, DLC allows for highly detailed tracking of multiple body parts within the same animal, providing richer and more precise behavioural data. At its core, DLC operates by fine-tuning a pre-trained deep convolutional neural network to perform pose estimation on user-defined keypoints. This process, illustrated in Figure 2.4, begins with manual annotation of a small subset of frames, where the experimenter labels the body parts of interest (*e.g.*

forelimb, snout, or tail base). These annotated frames are then used to train the network, and once the model is trained, it can be used to analyse new unseen videos and predict the location of the desired keypoints. The position of each keypoint is output as a pair of coordinates, accompanied by a likelihood value that reflects the network's confidence in the prediction. This likelihood threshold, referred to as *p-cutoff* during the training phase, can be used to exclude predictions below a defined confidence level and may also be adjusted later during post-processing, depending on the level of precision required for a specific analysis. Moreover, if the resulting likelihood values are unsatisfactory, the user has the option to relabel frames with low-confidence predictions and retrain the network, allowing the model to improve its accuracy and achieve better likelihood values across the dataset [2].

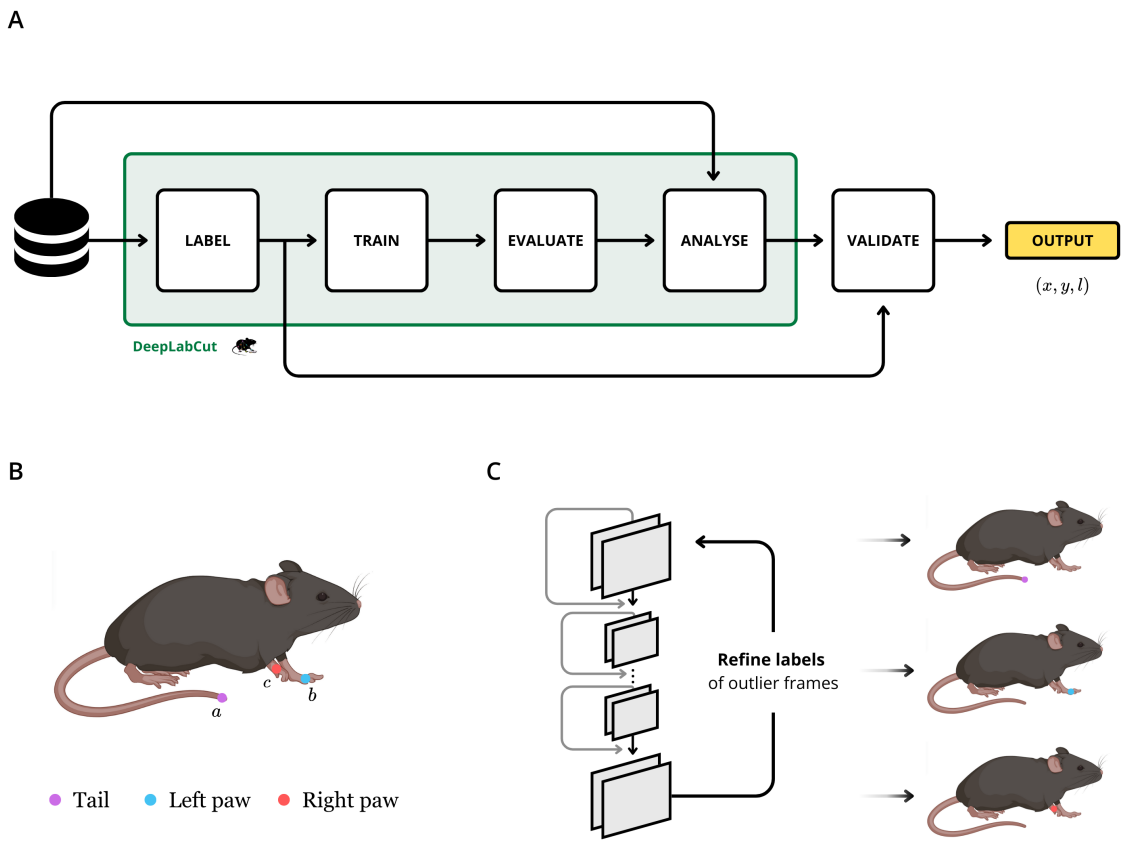

Figure 2.4: A –Schematic representation of the DeepLabCut workflow. B – Labelling process, exemplified with a mouse annotated with three keypoints. C – Network training process, with the possibility of relabelling outlier frames, which ultimately provides an output of coordinates for each keypoint.

Once the output from DLC has been obtained, it becomes possible to reconstruct the trajectory of these keypoints throughout the recorded session. This 2D trajectory data provides the basis for a wide range of downstream analyses, enabling the extraction of behavioural metrics that will be described in detail in Chapter 3.2.3.

While 2D pose estimation is sufficient for most behavioural studies, certain applications may require a higher level of spatial detail. In such cases, it is possible to use two or more camera angles to reconstruct the animal's movements in 3D space [37], [41]. This is typically achieved by first performing independent 2D pose estimation on each camera view, and then applying triangulation techniques to compute the three-dimensional coordinates of each keypoint. Anipose is one example of an open-source toolkit that enables this extension, building upon the 2D tracking outputs of DLC to generate accurate 3D pose reconstructions [41].

Besides their powerful analytical capabilities, both DLC and Anipose also provide intuitive visualisation tools that facilitate the inspection and interpretation of pose estimation results. DLC enables users to overlay predicted keypoints and skeletons directly on the original video frames, allowing researchers to qualitatively assess tracking accuracy. Similarly, Anipose extends these visualisation features to 3D, offering interactive plots where trajectories and postures can be explored from multiple angles.

Both cases are illustrated in Figure 2.5:

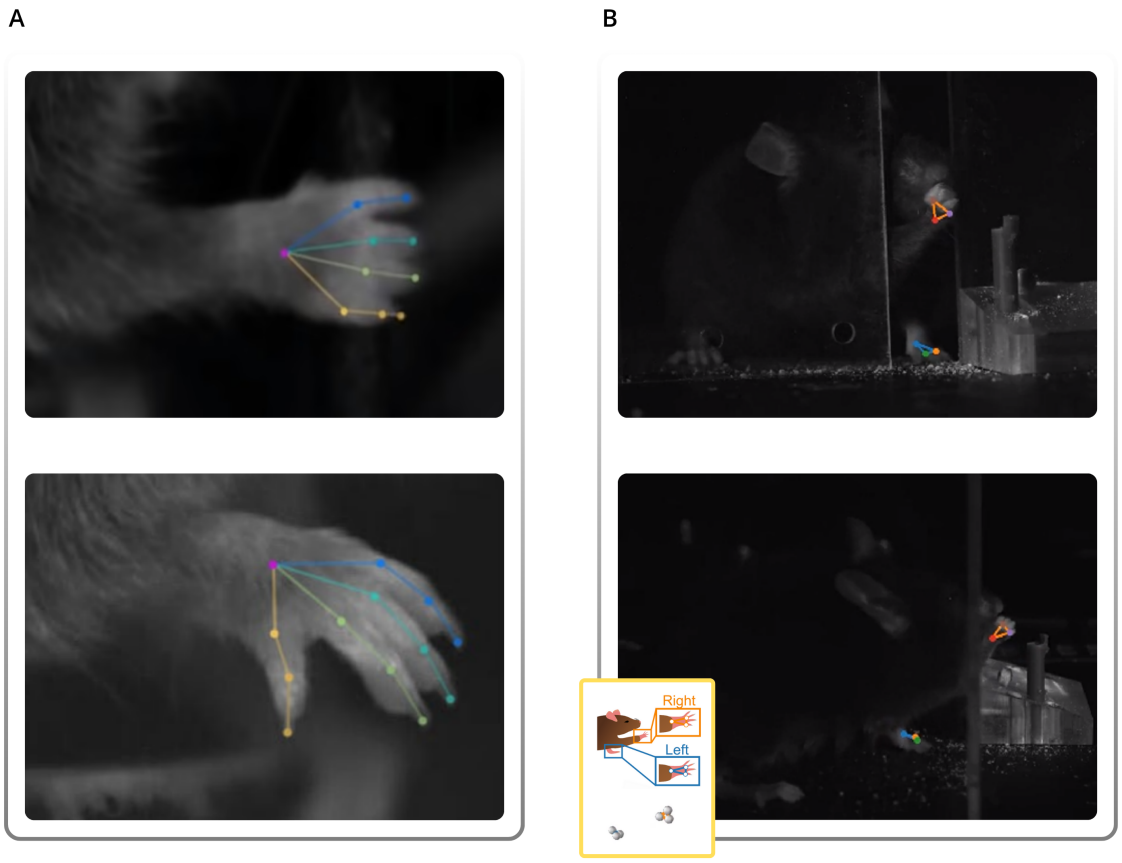

Figure 2.5: A – Visualisation of 2D pose estimation results in DeepLabCut, showing predicted keypoints overlaid on the original video frame. B – Visualisation of 3D pose estimation results in Anipose, showing predicted keypoints overlaid on the original video frames, allowing interactive exploration from multiple angles. Adapted from Mathis *et al.* [2] and Karashchuk *et al.* [41].

2.3.3 Experimental setups

Automated platforms for rodent motor behaviour have advanced considerably, with a particular focus on systems that can individualize task performance while enabling continuous operation. Such platforms allow each animal to engage in a specific task, such as reach-to-grasp, independently of others, supporting high-throughput behavioural assessment without constant human supervision.

An important contribution in this context was provided by Galiñanes, *et al.* [10], who implemented a water-based reaching task. Using liquid rewards instead of pellets allows a higher number of trials, with greater precision and fewer artefacts during movement, improving the reliability of behavioural measurements. This paradigm can be further enhanced by incorporating individualisation techniques, allowing each animal to perform the task independently while maintaining continuous monitoring, thus combining the advantages of high-throughput precision with personalised behavioural assessment.

An illustrative example of an individualised system is the high-throughput platform described by Salameh, *et al.* [11], shown in Figure 2.6. In this system, mice access a dedicated chamber connected to their home-cage to perform a pellet reach-to-grasp task, allowing continuous task engagement while recording detailed behavioural metrics. Each animal performs the task individually, identified through RFID (radio frequency identification) tagging. However, the design does not prevent other animals from intruding into the chamber while a mouse is engaged, potentially perturbing ongoing trials. Despite this limitation, the platform illustrates how modular systems can combine task-specific individualisation with continuous, flexible operation, supporting robust behavioural monitoring.

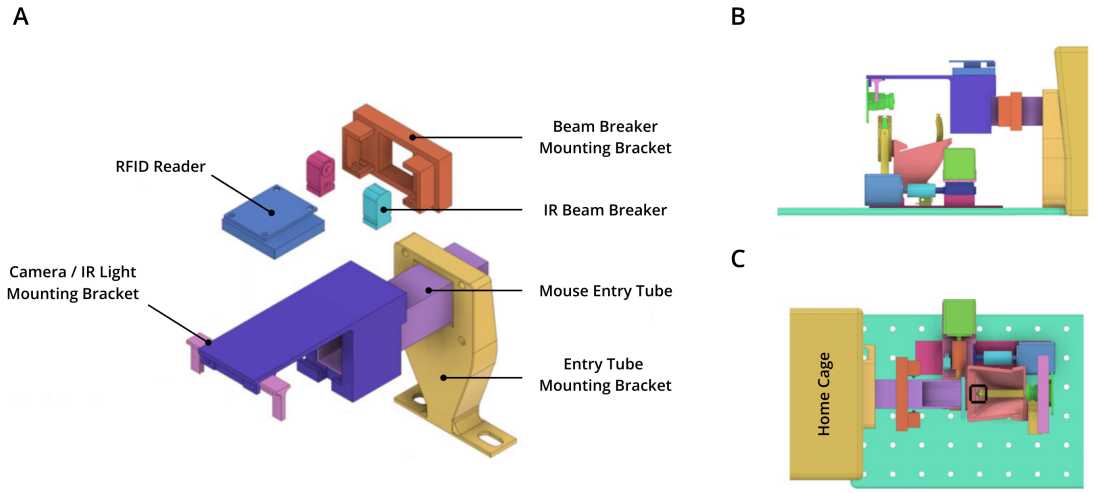

Figure 2.6: A – Exploded view of the apparatus connector system, highlighting the mouse entry tube that connects the home-cage with the reaching area. B – Side view of the full apparatus, showing the relative positions of the reaching compartment, seed arm, camera, and RFID tag reader for mouse identification. C – Top-down view of the full apparatus and the range of motion within which a seed could be presented (indicated by the black bounding box). Adapted from Salameh *et al.* [11].

To overcome the limitation of animals intruding into each other's testing chambers, several innovative approaches have been developed. Notably, Armshaw and Butcher recently shared their open-source apparatus, the one-rat turnstile (ORT) [42], [43], which was specifically designed for rats.

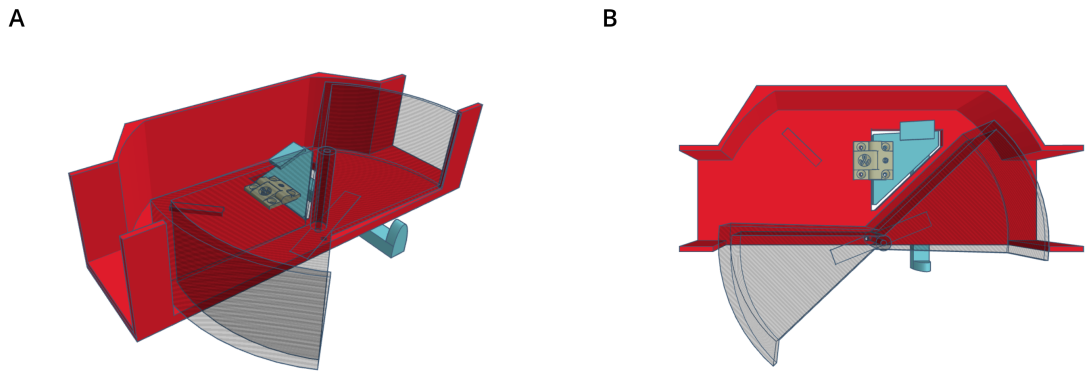

Figure 2.7: Isometric view (A) and top view (B) of the ORT module. The system base is shown in red, the turnstile mechanism in translucent grey, and the locking mechanism in blue. Secondary or support components have been omitted for clarity. The illustration was created in Tinkercad based on the file provided by Butcher *et al.* [43].

The ORT module, illustrated in Figure 2.7, integrates directly into the home-cage, allowing continuous individual monitoring, training, and testing without removing rats from their social environment. RFID technology tracks each animal, reducing human intervention while providing precise behavioural data, and the apparatus features a mechanism that unlocks the chamber door based on the weight of the rat on the turnstile, ensuring that only one animal can enter at a time. While adapting this weight-based strategy to mice is more challenging due to their smaller size, the underlying principle of the mechanism could be rethought to individualize access for mice. By automating data collection and preserving social dynamics, the ORT produces more reliable behavioural data while significantly reducing experimenter time and intervention.

2.4 Learning from dysfunction: applicability on movement disorders

The development of automated and scalable behavioural platforms holds broad relevance for the study of movement disorders. While different conditions present distinct motor abnormalities, they all require reliable methods to assess changes in precision, coordination, and adaptability. Traditional assays are often limited by low trial numbers, experimenter supervision, and simplified readouts that overlook the variability and subtlety of motor dysfunction. Automated setups, by contrast, enable continuous tracking of skilled forelimb actions across large cohorts, providing high-resolution and reproducible data while minimising experimenter bias. This makes them particularly suited to capture both progressive deterioration and subtle task-specific deficits that emerge only under demanding conditions.

Within this framework, reach-to-grasp paradigms are especially advantageous. They combine high motor demand with controlled, repeatable movements, allowing detailed kinematic analysis of planning, execution, and adaptation. When embedded into home-cage systems, these tasks not only increase throughput but also provide a translational bridge to better understand human pathophysiology and symptomatology, where similar skilled actions are commonly affected by neurological disorders. The integration of such tasks with modern interventions, such as optogenetics or pharmacological manipulations, further enhances their potential for dissecting the mechanisms of motor dysfunction.

2.4.1 Task-specific dystonia

To demonstrate the applicability of this approach, dystonia was selected as a representative case study. Dystonia is characterised by sustained or intermittent abnormal movements and postures that are typically patterned, repetitive, and often aggravated by voluntary action [44]. These symptoms can be categorised into multiple subtypes depending on clinical features, aetiology, and underlying mechanisms. Among them, task-specific dystonias stand out for their close association with the overuse of finely tuned motor skills, as exemplified by writer's cramp or musician's dystonia [45], [46], [47]. Their strong link to repetitive practice makes them a valuable model for exploring how sustained motor demand can trigger maladaptive changes in motor circuitry.

In this work, we combine behavioural triggers associated with task-specific dystonia and a genetic predisposition to the disorder. Specifically, we use a genetically modified model carrying the most common hereditary mutation, DYT-TOR1A, which results from a 3-base pair (ΔGAG) deletion in the TOR1A gene and causes the loss of a glutamate residue in the torsinA protein [48], [49]. By placing animals in an environment that encourages repetitive forelimb use for a specific action, we establish conditions that may reveal dystonia-like symptoms in genetically susceptible individuals.

Overall, the combination of automated monitoring, genetic predisposition, and behaviourally relevant

triggers provides a powerful strategy for investigating dystonia. More broadly, it exemplifies how the proposed platform can be applied to diverse movement disorders to uncover both shared and disorder-specific mechanisms of motor dysfunction.

2.5 Problem statement

Despite advances in behavioural neuroscience, a key caveat remains unresolved: the lack of reliable individualisation in automated paradigms. Most existing platforms cannot consistently identify and separate animals over extended periods, which severely limits their applicability for longitudinal studies in socially housed conditions. As a result, investigations often rely on short sessions, single-housed animals, or experimenter supervision, all of which reduce scalability and increase variability.

The present work addresses this gap by developing an automated water-based RtG platform designed around stable individualisation. By ensuring that each mouse can be consistently identified and monitored across long timescales, the system enables true longitudinal assessment of motor behaviour in group-living animals. Moreover, the use of a liquid reward paradigm inherently supports a high number of repetitions within each session. This property is particularly relevant as it allows us to obtain more iterations of the same movement, increasing the behavioural dataset and enhancing the statistical power of analyses.

This approach fills a critical gap between conventional assays and the need for scalable, individualised, and continuous monitoring of skilled motor control, providing a powerful framework for studying the progression and variability of movement disorders such as dystonia.

Chapter 3

Methodology

This chapter is organised by methodological components, progressing from the technical development of the system to the application of kinematic analysis tools, and finally to the description of the experimental procedures.

The development of the RtG setup, presented in Section 3.1, was undertaken entirely from scratch, representing the principal objective of this dissertation. This section details the major iterations of the setup, the integration of custom hardware components, and the design logic underlying the automatisation processes, highlighting how each modification contributed to achieving a fully functional experimental setup. Section 3.2 then focuses on the tracking and analysis of forelimb movements with DLC, primarily as a means to validate the setup. Finally, Section 3.3 describes the experimental procedures, which were designed both to troubleshoot and refine different stages of the setup, providing a thorough validation of its functionality and practical applicability.

All experiments and procedures performed during this work were performed in accordance with the Champalimaud Foundation Animal Welfare and Ethics Review Body and the Portuguese National Food and Veterinary Agency under license number 2020/013_A01; following the Portuguese Directive 113/2013 under the European Union Directive 2010/63/EU.

3.1 Setup development

3.1.1 Hardware

The development of the setup followed two main objectives: first, the construction and optimisation of the reaching chamber, and second, the design of a door mechanism to establish a reliable connection between the chamber and the animals' home-cage. Iterative improvements of the reaching chamber are described as versions 0.x, while versions 1.x correspond to successive iterations of the door mechanism

3.1.1.1 Version 0.0 - Reaching chamber prototype

The first iteration of the setup, illustrated in Figure 3.1, comprised a cubic reaching chamber ($10 \times 10 \times 10$ cm) made of 3 mm acrylic sheets with a slit aperture (9.5×20 mm, radius 4.75 mm) positioned in the front panel of the chamber, 34 mm above the chamber floor and shifted 10 mm from the right inner wall of the (from the animal's perspective). This slit was designed to allow the animal to fully extend the right forelimb while limiting the passage of the snout.

Water was dispensed through a stainless steel spout, horizontally aligned with the centre of the slit aperture, and connected to a Harp syringe pump [50], fitted with a 5 ml syringe. This syringe pump was

used due to its reliable delivery of liquid volumes in the microlitre range and its easy integration with Bonsai RX [33], [50]. Additionally, a custom 3D-printed spacer piece was developed and attached to the stainless steel spout to allow incremental adjustment of the water distance from the slit in 2 mm steps to fine-tune the ideal reaching distance.

To ensure stability, the reaching chamber was mounted on an acrylic support that prevented displacement during interaction and guaranteed consistent camera alignment across sessions, while allowing easy removal for cleaning between animals. All components were mounted onto a Thorlabs breadboard (30 $\times$ 30 cm), providing a rigid platform with standardised mounting holes for flexible assembly and reconfiguration.

To record the videos, this configuration also incorporated a single camera (Model Flea3 FL3-U3-13S2M, FLIR) recording at 200 fps, triggered via Bonsai RX [33], along with a mirror positioned at 45º relative to the camera's viewing axis, enabling the acquisition of a frontal view of the reaching behaviour.

For illumination, multiple LED strips were mounted behind the camera to provide uniform lighting of the reaching movements.

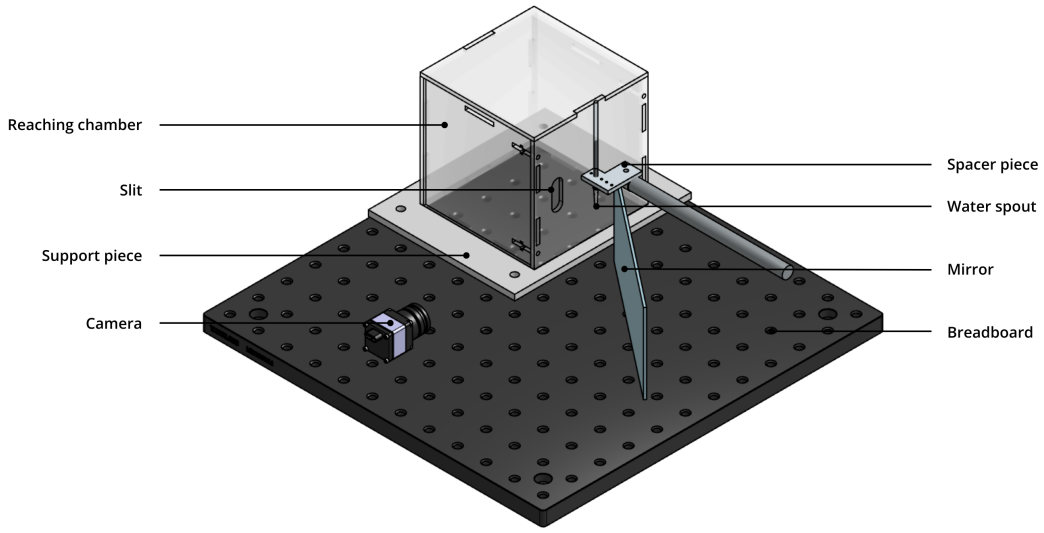

Figure 3.1: Version 0.0 of the RtG setup. Support pieces were omitted to improve visibility.

3.1.1.2 Version 0.1 - Slit repositioning and camera adjustment

In Version 0.1, several features were retained from Version 0.0 including most chamber dimensions and design, the water delivery system, and the custom 3D-printed spacer mechanism. However, two key structural modifications were introduced, as seen in Figure 3.2, to optimise the camera's field of view and promote consistent use of the right forelimb.

First, the slit aperture was repositioned to the left side of the front panel, placed 10 mm from the inner left wall of the chamber (from the animal's perspective), and its height increased to 25 mm, while maintaining the original width and corner curvature (9.5 mm and radius 4.75 mm, respectively). The vertical position of the slit remained unchanged at 34 mm from the chamber floor.

To accommodate the new slit position, the mirror had to be reoriented and the focal length of the camera was adjusted.

Second, the water spout, was gradually displaced leftward and was ultimately positioned 5 mm off-centre relative to the slit aperture. This spatial asymmetry was intended to bias forelimb choice and

successfully encouraged consistent right paw usage across all subjects, thereby ensuring alignment with the recording axis and full visualisation of the limb.

Additionally, minor modifications were introduced to improve video quality. The LED strips were replaced with infrared lighting, and multiple light source positions were tested to optimise illumination conditions and minimise reflections or shadows in the recorded videos.

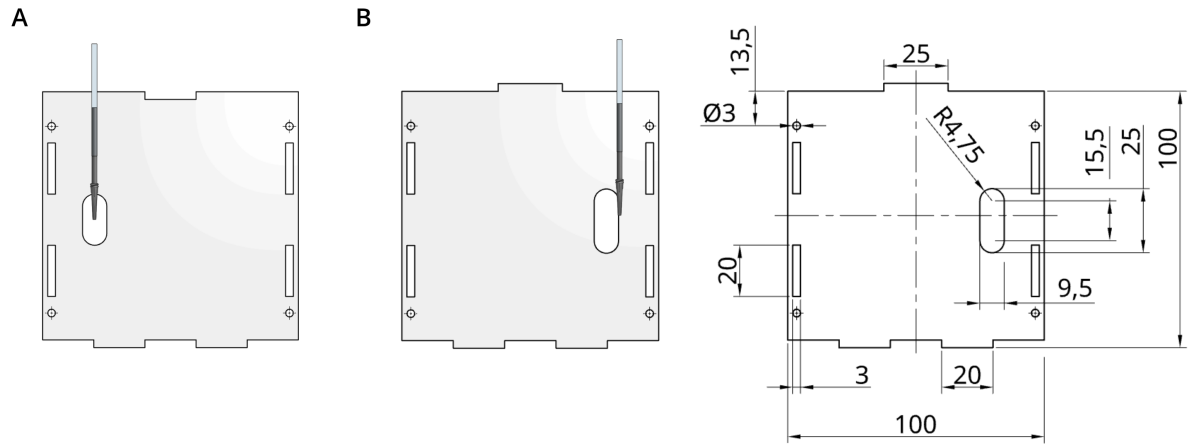

Figure 3.2: Front panels of the reaching chamber in Version 0.0 (A) and 0.1 (B), showing the modifications introduced in this configuration. All dimensions are drawn to scale and expressed in millimetres

3.1.1.3 Version 0.5 - Final reaching chamber

Version 0.5, illustrated in Figure 3.3, preserved the core features described in Version 0.1, including the chamber dimensions, slit aperture geometry and position, and the overall mirror–camera configuration. The water spout remained aligned with the slit and positioned 5 mm off-centre to reinforce right paw use.

The principal modification in this version was the replacement of the 3D-printed spacer with a linear actuator (Actuonix L12-I), which provided automated and continuous control over the distance between the water spout and the slit. This innovation eliminated the need for manual adjustments between sessions and enabled fine-tuning of the spout position within a single session, which is particularly important during the early training phase when animals are learning the reaching task.

Additionally, the top panel of the chamber was redesigned to accommodate wired connections for parallel experiments, such as *in vivo* calcium imaging and electromyography (EMG) recordings. For EMG measurements, an aluminium foil layer on the chamber floor was added to reduce electrical noise and provide a reliable ground reference. Lateral stoppers were also incorporated to prevent any accidental lifting of the top panel, ensuring stability and animal safety throughout the session.

Illumination was optimised to guarantee clear visibility of the water droplet. A dedicated LED was positioned directly above the spout, while the overall chamber lighting relied on a single infrared spotlight, stripped down to its essential components to minimise electrical noise. A black acrylic panel was placed in front of the infrared spotlight to reduce light scattering, focus illumination on the chamber, and minimise unwanted reflections.

Furthermore, the camera frame rate was increased from 200 fps to 250 fps through minor downscaling of the recording resolution, allowing more precise capture of rapid forelimb movements.

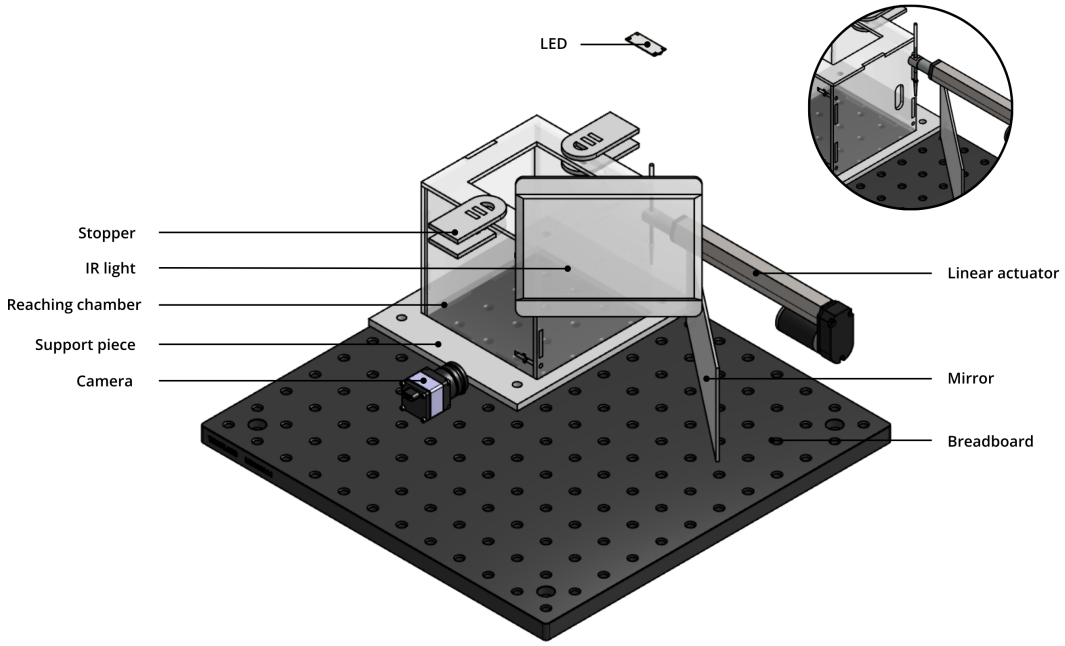

Figure 3.3: Version 0.5 of the RtG setup. The magnified area displays the slit and the water spout. Support pieces were omitted to improve visibility.

3.1.1.4 Version 1.0 - RFID-controlled door

Version 1.0 consists of a physical passage connecting the reaching chamber (Version 0.5) to the home-cage, incorporating an RFID-based identification and access-control system.

The passage consisted of a tunnel equipped with a rotary door driven by a top-mounted servo motor (KST DS215MG). An RFID sensor was positioned centrally at the upper section of the tunnel to detect implanted RFID tags. Upon detection, the sensor output triggered the servo motor, rotating the door and enabling access between the compartments. The specific design of the rotary door included an integrated side wall that blocked the tunnel from one side while opening it on the other, ensuring that only a single animal could pass at a time while physically preventing access from other individuals during the transition.

Multiple hardware variants of this design were fabricated to allow flexibility in system testing:

- Open tunnel: completely unobstructed, allowing unrestricted passage for training and habituation.
- Passive rotary door: mounted on the same axis as the active system but without servo actuation, allowing animals to push the door manually (also for training).
- Active servo-driven rotary door: actuated upon RFID detection, providing controlled access between the home-cage and the reaching chamber.

All components were designed and mounted in a modular fashion, allowing individual elements such as tunnel sections, sensors, or door mechanisms to be rapidly replaced or reconfigured during iteration. Power and control signals for the servo and RFID module were routed externally to simplify maintenance and potential adjustments.

These variants are illustrated in Figure 3.4, which shows the open tunnel (A) and the active servo-driven door (B), as well as a schematic of a mouse passing through it (C). The passive door corresponds to the same setup as in B, differing only by the absence of the servo and RFID sensor.

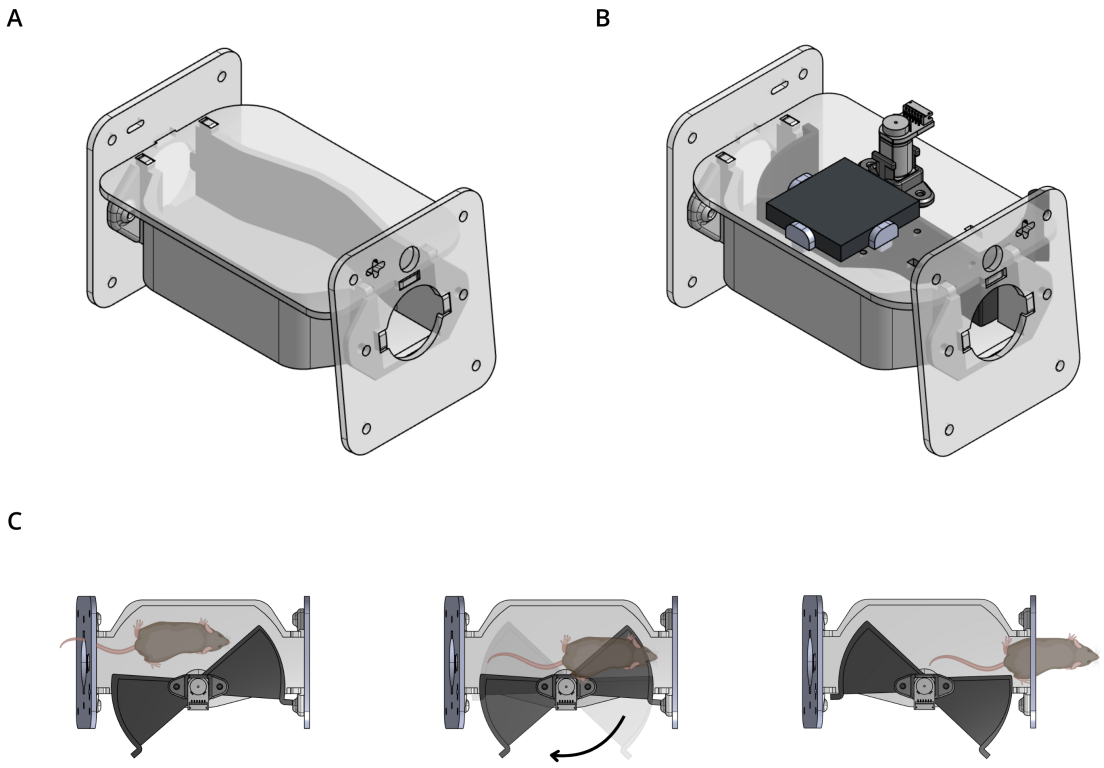

Figure 3.4: Schematic representation of the door mechanism in Version 1.0. A – Open Tunnel. B – Active servo-driven door. C – Mouse passing through the door mechanism.

3.1.1.5 Version 1.1 - RFID-controlled stopper

Version 1.1 constituted a significant improvement over Version 1.0, maintaining the primary goal of individualising and identifying animal passages while introducing a more effective control mechanism.

However, unlike the automated RFID-controlled door used in Version 1.0, this version employed a passive door system that animals could physically push to move between compartments, while restricting access to one animal at a time.

This change was driven by several observations in the automated door system of Version 1.0, which are discussed in Section 4. Consequently, we implemented a mechanical stopper system that physically blocked or released the door based on the animal's position. By allowing animals to push the door manually once unblocked, the system promoted more natural behaviour and smoother transitions between compartments, thereby minimising stress and hesitation during access.

This stopper mechanism, illustrated in Figure 3.5, consisted of a 3D-printed component featuring an external compartment and a bevelled edge that moved upwards when pushed and returned downwards under the influence of gravity. The 3D-printed piece was connected to a rotary servo motor (Hitec HS-422), which alternated between two positions separated by 180º.

When the stopper was oriented in one position, it allowed the animal to push the door towards the reaching chamber by lifting the bevel, which subsequently blocked the door behind the animal. Conversely, to return to the home-cage, the servo rotated the stopper to the opposite position, enabling the

animal to push the door back, again raising the bevel and locking the door thereafter. The operational logic of the servo control is later detailed in Section 3.1.2.7.

As illustrated in Figure 3.5 (and in Appendix C), multiple hardware variants were fabricated for training and testing purposes:

- Open tunnel: completely unobstructed, allowing unrestricted passage for habituation and training.
- Passive rotary door: permitting animals to manually push the door without blockage from the stopper system.
- RFID stopper system: integrating the mechanical stopper described above, controlled via RFID detection to individualise and regulate animal access.

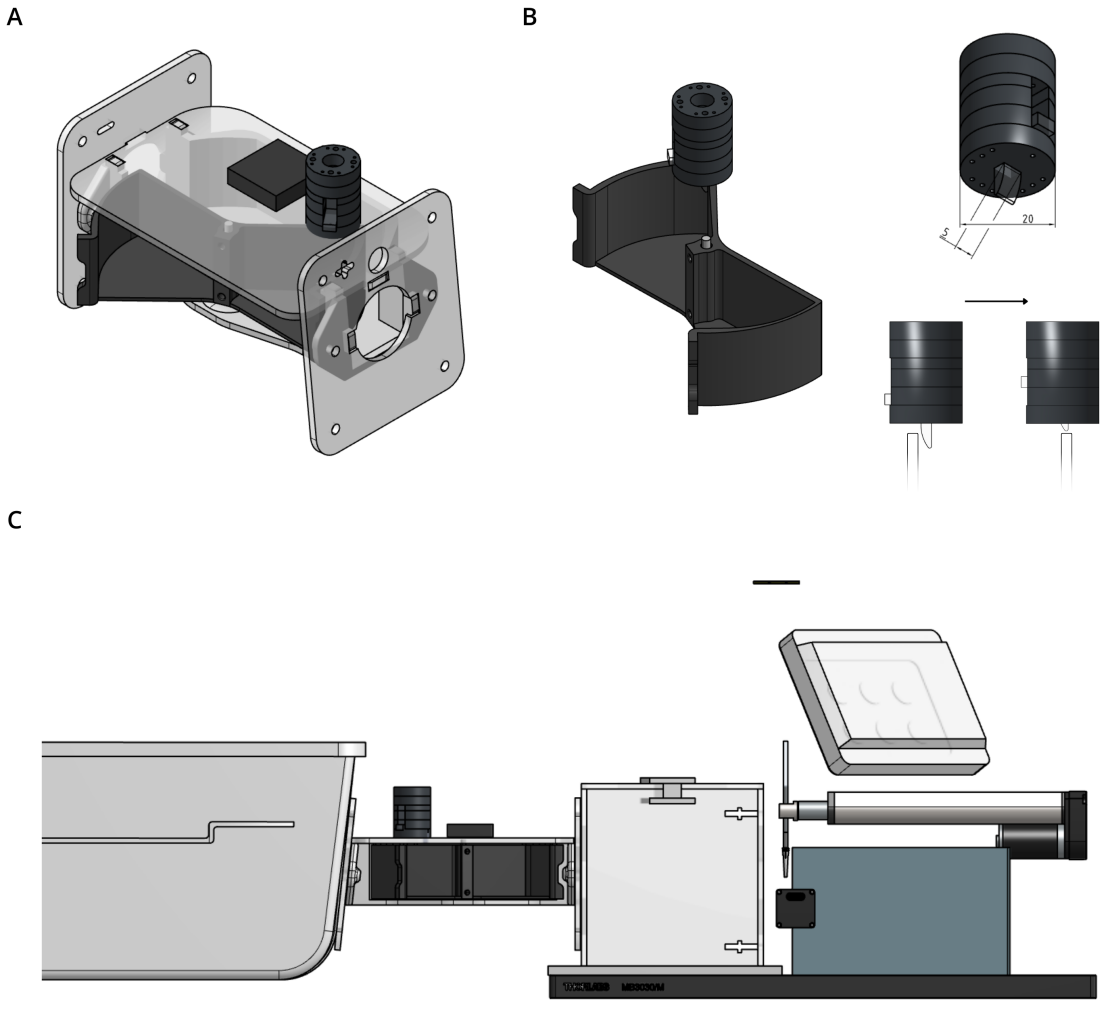

Figure 3.5: Version 1.1 of the RtG setup. A – Door mechanism with the RFID-controlled stopper system. B – Stopper system and its interaction with the door, where the bevelled piece allows the animal to enter when pushed in one direction and blocks passage when pushed in the opposite direction. C – Final RtG setup, incorporating the reaching chamber, the door mechanism, and the home-cage.

3.1.2 Software

This section outlines the key components and automatised processes that support the functioning of the experimental setup. All processes were implemented using Bonsai RX, which was initiated through

the Python workflow described in subsection 3.1.2.1.

3.1.2.1 Session initialisation and data logging

To initiate each session, a Python script was developed to define the configuration of multiple parameters, such as the animal ID, animal weight, actuator position, script version and session duration. Once these inputs are defined, the script launches the appropriate Bonsai RX workflow and prepares the system for acquisition.

During each session, multiple streams of data are recorded and synchronised to ensure comprehensive tracking and analysis. This includes a complete list of all acquired frames to guarantee that no frames are lost during acquisition, the full set of behavioural board metadata, all recorded video clips, and the precise frame indices associated with each clip; this detailed logging enables accurate temporal alignment of specific clips with complementary experimental techniques and data files. Additionally, extracted behavioural metrics are logged continuously in a history file specific to each animal, facilitating longitudinal tracking of parameters such as the number of task repetitions, video acquisitions, and water drops delivered throughout the session.

All session-related outputs, including video files, extracted metrics, behavioural metadata, and configuration settings, are automatically organised and saved within a structured folder hierarchy assigned to each animal. This systematized data management facilitates efficient access, reproducibility, and traceability for subsequent analysis.

3.1.2.2 Water delivery

To ensure precise and consistent water delivery throughout the behavioural task, a visual detection system was implemented using continuous image monitoring. Specifically, an region of interest (ROI) is defined beneath the dispensing tip, and the average pixel intensity (API) within this region is computed in real time.

This method relies on the optical contrast between the background and the presence of a water droplet: when a droplet is present, the API within the ROI increases, whereas its absence results in a lower value. The API, denoted as $\bar{I}(t)$, is computed by continuously monitoring the pixel intensity $I(t)$ over time, and is given by:

$$\bar{I}(t) = \frac{1}{N} \sum_{i=1}^{N} I_i(t) \tag{3.1}$$

Here, $I_i(t)$ is the greyscale intensity of the i^{th} pixel in the ROI, and N is the total number of pixels in that region.

$\bar{I}(t)$ is then compared to a predefined threshold T, which serves as a criterion for droplet presence detection and delivery control. The decision process is formalised as:

$$\text{Action}(t) = \begin{cases} \text{Deliver droplet}, & \text{if } \bar{I}(t) < T \text{ for } \Delta t \geq 1 \text{ s} \\ \text{No action}, & \text{if } \bar{I}(t) \geq T \end{cases}$$

To maintain detection accuracy when the dispensing tip position changes, the system automatically updates the ROI according to the actuator movement. Since background contrast may also vary with tip position, the threshold value T is dynamically adjusted for each new ROI.

3.1.2.3 Water refill

Because Harp syringe pumps offer high precision but are not designed for very large syringes, it was necessary to implement an auxiliary protocol to enable continuous operation over extended periods. To ensure uninterrupted droplet delivery, the system therefore incorporates an automatic refill mechanism. A counter tracks the total number of droplets delivered and when this counter reaches a predefined limit L, the system temporarily suspends droplet delivery and enters refill mode.

In this mode, the solenoid valve switches its position to disconnect the syringe pump from the dispensing tip and instead connect it to an external water reservoir. Once the connection is established, the syringe is refilled to 100% of its capacity. Upon completion, the valve returns to its original position, reconnecting the syringe pump to the dispensing tip, at which point the droplet delivery protocol resumes and the counter is reset to zero.

Although the reservoir–syringe interface is ideally a closed system, small air bubbles occasionally appeared in the fluidic path. To prevent the system from misinterpreting air expulsion as droplet delivery, an additional step was introduced immediately after each refill. In this step, the syringe pump is actuated for a number of steps corresponding to approximately ten droplets, ensuring that any residual air is expelled and that the delivery tip is primed with water, thus avoiding delays in resuming normal operation.

3.1.2.4 Video capture

To capture videos efficiently, an approach focused on optimising storage space was necessary. Since the ultimate goal was to operate the setup continuously over several hours or days, recording full-length videos was impractical. Instead, the videos were segmented into short clips.

A method similar to that described for the identification of a water droplet with an ROI (in Section 3.1.2.2) was implemented. In this case, the region of interest was defined between the slit and the dispensing tip, allowing detection of the animal's paw as it attempted to reach for the water. An increase in the API within this ROI indicated that the paw was crossing the region, triggering the command to record a video clip.

To ensure the complete reaching movement of the animal was captured, a buffering mechanism based on a delayed live video stream was implemented. Specifically, the live video feed is delayed by a time interval d, so that when a recording command is triggered by the detection of the paw entering the ROI, the system saves a clip starting from d seconds before the command was issued and lasting for a total duration $D = 2d$. This means the clip contains both the moments preceding and following the trigger, capturing the full reach motion.

Furthermore, after a recording command is issued, the system maintains the delay d before it can accept a new recording command, preventing overlap between clips and ensuring continuous movements are fully recorded without loss. This buffering and delay strategy creates a seamless capture of consecutive reaching events even if they occur in rapid succession.

In this specific case, since clips of duration $D = 3\,\mathrm{s}$ were used, the delay was set to $d = 1.5\,\mathrm{s}$.

3.1.2.5 Identification of animals

In both Version 1.0 and Version 1.1 of the setup, it is essential to identify which animal is passing through the tunnel. To achieve this, an RFID reader was employed. This device not only detects which

animal is entering the reaching chamber but also enables the implementation of access protocols based on the information read.

Each animal is implanted with a unique RFID chip, which is automatically associated with its identification number within the system. Upon detection, the RFID reader communicates the chip ID to the control software, which then updates the relevant CSV files, as described in Section 3.1.2.1, by logging the specific identification number of the animal at each detected event. This process ensures accurate tracking and individualisation throughout the experimental sessions.

3.1.2.6 RFID-controlled door system

To control the door mechanism described in Version 1.0, a workflow was implemented in Bonsai RX to automatically rotate the door in either direction based on the information received from the RFID reader. The incoming signal from the reader was continuously monitored and processed using a temporal filter to avoid false positives caused by brief or partial detections. When the RFID chip was detected for a minimum duration t_{detect}, the servo motor was commanded to rotate the door to the opposite position, granting passage. Safety delays were introduced between consecutive activations to prevent oscillatory behaviour or repeated triggering when the same animal remained in the detection zone. This control logic was later reused in a subsequent version of the setup.

An encoder was also integrated into the system to track the exact angular position of the door. This allowed the workflow to make real-time decisions based on whether the door was currently open, closed, or in transit, enabling the implementation of position-dependent logic such as blocking new commands while the door was moving. This approach was not fully explored due to technical issues encountered in Version 1.0, which are described in Chapter 4.

3.1.2.7 RFID-controlled stopper system

To control the stopper described in Version 1.1, a workflow was developed in Bonsai RX that enabled blocking or unblocking the door based on the information received from the RFID reader. A stopper alternated between two states, denoted as *entry free* and *exit free*. In the *entry free* state, the door was unlocked to allow the animal to enter from the home-cage to the reaching chamber but remained locked in the opposite direction. Conversely, in the *exit free* state, the door was unlocked to permit the animal to exit the reaching chamber and return to the home-cage, while locked in the reverse direction.

The stopper switched states only when the animal's RFID chip was continuously detected by the reader for a minimum duration of $t_{\text{detect}} = 2\,\text{s}$. This interval was intended to motivate the animal to push the door and to prevent false positives caused by rapid back-and-forth movements through the tunnel.

A key aspect of the control logic involved maintaining a counter C that incremented each time the stopper rotated between states. This counter was essential to track the current state of the stopper: when C was odd, the system was in the *entry free* state, allowing entry to the reaching chamber; when C was even, it was in the *exit free* state, allowing exit back to the home-cage.

Based on this counter, a minimum dwell time t_{min} was enforced to ensure that the animal remained in the reaching chamber long enough to perform the RtG task multiple times. Specifically, after entering the chamber (*i.e.*, when C became odd), the system prevented switching the stopper back to the *exit free* state (*i.e.*, incrementing C to an even number) until the elapsed time exceeded t_{min}. This prevented premature door unlocking and ensured sufficient task engagement. The optimal value implemented for this delay was set to $t_{\text{min}} = 3\,\text{min}$.

3.2 Kinematic analysis

3.2.1 Pre-processing

Given that our recordings included both a frontal and a lateral view of the RtG task, it was necessary to split each video into two corresponding view-specific files prior to analysis with DLC. To achieve this, we adapted an interactive script kindly provided by Simon Zamora (Champalimaud Foundation), which allowed visual inspection and manual adjustment of the cropping boundaries. Once the limits were defined, the script automatically processed all videos, generating two separate files per recording. The output was organised into a set of directories following the structure described in Section 3.1.2.1, with each file labelled with its respective animal and view.

3.2.2 DeepLabCut

After pre-processing and view splitting, pose estimation was performed using DLC (version 2.3.10) [2], [37]. The following section describes the full pipeline used for labelling, network training, evaluation and the generation of final outputs used in downstream analyses.

3.2.2.1 Frame extraction and labelling

At first, a representative subset of the dataset was selected for training and validation. From 48 videos corresponding to 24 animals, we extracted a total of 960 frames to form the labelling pool. Frames were randomly selected while ensuring they were equally spaced within each video. This approach avoided excessive redundancy and ensured that a broad range of poses and illumination conditions was represented, reducing the risk of overfitting to specific video segments.

Selected frames were manually annotated using the DLC graphical user interface, where we defined 12 keypoints (as seen in Figure 3.6): the nose, the centre of both ears, and on the right forelimb the shoulder, elbow, wrist, centre of the paw, and the tip of three digits excluding the thumb and little finger. Additionally, the centre of the left paw and the water droplet were annotated.

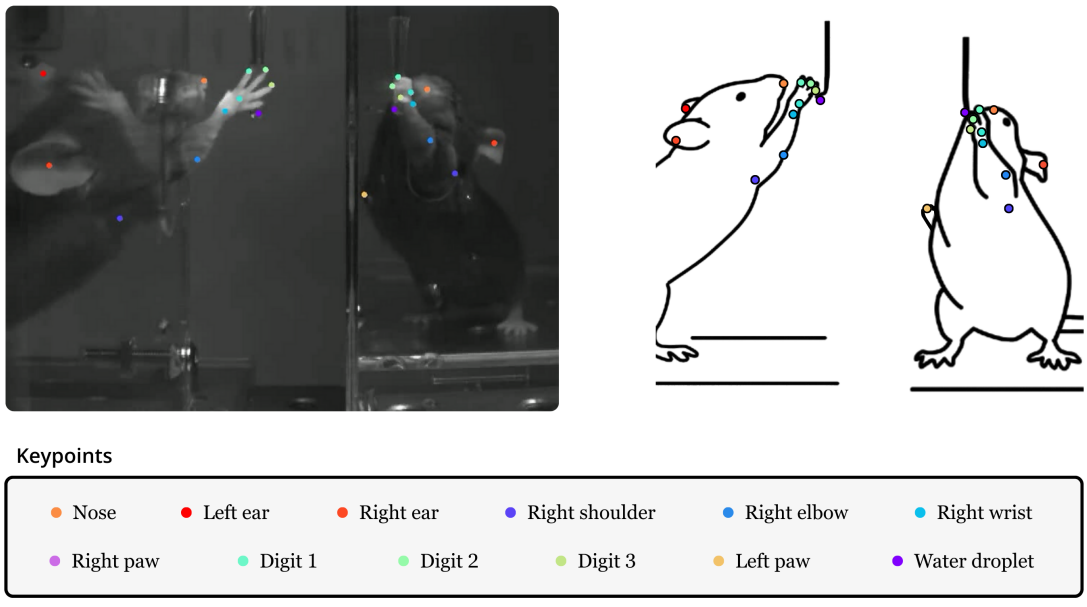

Figure 3.6: Real video of a mouse performing the task and schematic representation of the corresponding annotated keypoints used for motion tracking. The frontal view appears inverted due to the use of a mirror.

These keypoints were chosen to capture different aspects of the behaviour: the head landmarks (nose and ears) provide a reference for posture and orientation, the right forelimb markers allow precise tracking of the reaching kinematics, the digits offer a measure of fine motor control, and the left paw serves as a control reference for bilateral movements. Each keypoint was labelled in every selected frame when visible, as illustrated in Figure 3.6, while occluded or ambiguous points were left unlabelled. The resulting labelled dataset thus consists of images paired with corresponding keypoint coordinates and was visually inspected to ensure annotation consistency across animals and views.

3.2.2.2 Network training, evaluation and analysis of new videos

The labelled images were assembled into a DLC project and split into training and testing subsets. We used a random split of 95% for training and 5% for testing and no additional image pre-processing was applied prior to training, since DLC accepts raw video frames and performs internal augmentation. We then used a ResNet-50-based neural network [51][52] with default parameters for 600000 training iterations. Using a *p-cutoff* value of 0.6 we obtained a training error of 4.52 pixels and a test error of 5.80 pixels. Note that this threshold was treated as a flexible parameter so it could later be adjusted on a per-metric basis during post-processing analysis. While these error values provide confidence in the predictions of our trained model, we still chose to improve the network by performing an iterative relabelling cycle. Low-confidence frames were added back to the labelling set, re-annotated, and the network was retrained. This iterative strategy enhanced robustness and led to improved performance, resulting in a training error of 2.98 pixels and a test error of 4.12 pixels

Once we were satisfied with the performance of our trained network, it was used to analyse new, unseen videos. Each video frame was processed to predict the defined keypoints, producing data for further analysis.

3.2.3 Post-processing analysis

Following the predictions generated by the trained network, a post-processing pipeline was implemented to ensure that the recorded data could be reliably transformed into meaningful insights depending on the experimental objective. At this stage, the analysis is exploratory and preliminary in nature, focusing primarily on validating the quality and consistency of the acquired data rather than on the final interpretation. This approach allows us to confirm that the setup and tracking pipeline provide robust outputs suitable for subsequent applications.

In this analysis, each RtG movement was considered as a complete unit, from the moment the forelimb crossed the slit until it returned to the cage. Although this segmentation captures the full action, it could also be subdivided into distinct phases, such as reaching and retrieval, depending on the desired resolution of future analyses.

To confirm that the extracted outputs allow us to distinguish relevant examples depending on the analytical focus, several exclusion criteria were tested and applied. First, vain reaches were discarded, defined as movements in which the water droplet was absent in the beginning of the clip. To avoid biases from repeated attempts, only the first reach within each clip was retained. Furthermore, reaches were defined as starting when the paw's centre crossed the slit and ending upon retraction. Additionally, a minimum distance threshold was imposed to exclude incomplete attempts where the animal inserted and withdrew the paw almost immediately.

Because the experimental design involved different distances between the slit and the water droplet, a distance normalisation procedure was also considered. In this case, the paw trajectory was normalised

to the Euclidian distance between the slit and the droplet position, ensuring comparability across trials. Consequently, velocity and acceleration metrics could also be computed in a normalised form. It is important to note that this normalisation step is optional and can be adapted depending on the analysis goals.

Based on the filtered and normalised trajectories, additional kinematic features were extracted. The paw trajectory was calculated and differentiated to obtain velocity and acceleration profiles. These metrics provided the foundation for a range of quantitative parameters:

Following the extraction of filtered and normalised paw trajectories, several kinematic parameters were computed as potential proxies for movement characteristics. Each metric provides an initial, exploratory insight into the behaviour and precision of the reaching movements. The formal definitions are provided below:

Reaching time evaluates movement duration and it is defined as the interval between the paw crossing the slit and its retraction:

$$T_r = t_f - t_0 \tag{3.2}$$

Here, t_0 represents the frame at which the paw crosses the slit, and t_f corresponds to the frame at which the paw retracts after a minimum elapsed time. If one wants to analyse the time to reach the droplet, t_f instead corresponds to the frame at which the droplet disappears. All time measurements refer to frames and can be consequently converted to seconds, in this case, 250 frames = 1 s.

Path efficiency reflects how direct the paw movement is from slit crossing to retraction, providing an indicator of movement straightness:

$$E_p = \frac{||\mathbf{p}(t_f) - \mathbf{p}(t_0)||}{\sum_{t=t_0}^{t_f} ||\mathbf{p}(t+1) - \mathbf{p}(t)||} \tag{3.3}$$

Here, $\mathbf{p}(t)$ is the paw position vector at frame t, and the denominator represents the total path length until retraction.

Velocity-related features are potential indicators of movement dynamics. The peak velocity and the frame at which it occurs are given by the following equations, where $\mathbf{v}(t)$ is the paw velocity vector at frame t:

$$v_{\max} = \max(||\mathbf{v}(t)||) \qquad t_{\text{peak}} = \arg\max_t ||\mathbf{v}(t)|| \tag{3.4 and 3.5}$$

Movement Smoothness provides a measure of movement fluidity by quantifying how consistently acceleration changes over time. In our analysis, movement smoothness $\mathbf{S}(t)$ is defined as:

$$\mathbf{S}(t) = \frac{1}{|\mathbf{a}(t)|} \tag{3.6}$$

Here, $\mathbf{a}(t)$ represents the acceleration of the paw at time t, computed as the derivative of the paw velocity $\mathbf{v}(t)$. Higher smoothness values indicate more gradual changes in acceleration, reflecting more fluid and coordinated movements, while lower values correspond to abrupt or irregular motion patterns.

Initial direction error provides a proxy for the accuracy of movement initiation. It is computed as the angular deviation between the ideal trajectory vector (a straight line connecting the slit opening and the droplet position) and the actual movement vector over the first 30 frames:

$$\theta_{\text{error}} = \arccos \frac{\mathbf{d}_{\text{ideal}} \cdot \mathbf{d}_{\text{actual}}}{||\mathbf{d}_{\text{ideal}}|| \, ||\mathbf{d}_{\text{actual}}||} \tag{3.7}$$

Here, $\mathbf{d}_{\text{ideal}} = \mathbf{p}(t_f) - \mathbf{p}(t_0)$ is the ideal displacement vector, and $\mathbf{d}_{\text{actual}}$ is the vector representing the paw displacement over the first 30 frames.

Endpoint variability acts as a possible measure of movement consistency and is defined as the dispersion of final paw positions across trials:

$$\sigma_{\text{end}} = \sqrt{\frac{1}{N} \sum_{i=1}^{N} ||\mathbf{p}_i(t_f) - \overline{\mathbf{p}}(t_f)||^2} \tag{3.8}$$

Here, N is the number of trials, $\mathbf{p}_i(t_f)$ is the final paw position in trial i, and $\overline{\mathbf{p}}(t_f)$ is the mean final position across trials.

Together, these parameters provide a first-level validation of the system's ability to capture and quantify forelimb movements with high precision. While the current focus remains on assessing data robustness and pipeline reliability, the same framework can later be adapted for more detailed behavioural interpretations.

All data processing and subsequent analyses were performed using Python.

3.3 Experimental procedures

Throughout the development of this project, a series of experiments were conducted with the aim of validating and optimising the behavioural setup. These experiments, described in the following subsections, were designed to progressively test different aspects of the system, from basic operability and task feasibility to long-term stability.

Animal handling was carried out by Madalenna Bettencourt, Filipa França de Barros, Joaquim Alves da Silva, Elisabetta Saccone, Joseph Tutt, Simon Zamora, and Pedro Dias (Champalimaud Foundation).

3.3.1 Early-prototype experiment

3.3.1.1 Animals

A total of 6 mice (2 DYT1 knock-in mutants (DYT) and 4 wild-type (WT) littermate controls) were included in the early-prototype experiment, with their individual characteristics summarised in Table 3.1.

Mice were kept in a light/dark cycle with Zeitgeber Time 0 at 8:00 AM in a separate temperature-controlled room (21.0 ± 2.0 ºC) with food provided *ad libitum*. Due to the nature of the experiment, mice were water-deprived one day before the sessions began and subsequently had access to water only during the experimental periods, with a maximum allowed intake of 1 ml per session. The experiment was conducted five days per week and on non-experimental days, 1 ml of water was provided per animal to maintain hydration without interfering with behavioural performance. All the experiments were performed during the light part of the cycle, with approximately 24 hours between sessions. Animals were

weighed before each session to monitor their condition and ensure their welfare.

Table 3.1: Animal cohort details for the early-prototype experiment.

Mouse ID	Sex	Genotype	Surgical condition	Starting weight (g)	Age (weeks)
4812	♂	WT	—	30.5 ± 0.1	15
4813	♂	WT	—	31.9 ± 0.1	15
4814	♂	DYT	—	30.4 ± 0.1	15
4815	♂	WT	—	30.1 ± 0.1	15
4937	♂	WT	—	28.9 ± 0.1	11
4939	♂	DYT	—	30.3 ± 0.1	11

Note. Starting weight refers to experimental day 1 (*i.e.*, after water deprivation). Starting age indicates the number of full completed weeks at the beginning of the experimental protocol. WT – wild-type; DYT – heterozygous carrier of the DYT1 mutation; ♂ – Male; ♀ – Female.

3.3.1.2 Protocol

This experimental phase aimed to validate the first functional version of the reaching chamber and assess the feasibility of water delivery and video acquisition automatization.

The experiment was conducted over a four-week period (Figure 3.7), beginning with an initial phase of training and habituation, followed by kinematic assessment across three consecutive weeks.

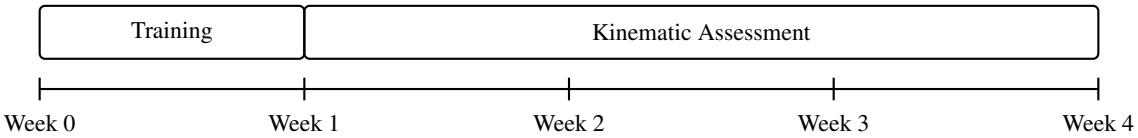

Figure 3.7: Schematic representation of the early-prototype experimental timeline.

Each session lasted approximately 15 to 20 minutes per animal, depending on task engagement, with mice typically performing until they reached the daily water limit of 1 ml. In cases of particularly high engagement, this limit was slightly exceeded, with the session terminating at the 20-minute mark. Version 0.0 of the setup was used until week 2, after which Version 0.1 was employed until the end of the experiment. Session initialisation, water delivery, and video capture were automated following earlier versions of the protocols described in Sections 3.1.2.1, 3.1.2.2, and 3.1.2.4.

During the training phase, 10 μl water droplets were delivered to the animals, and the tip was gradually positioned further from the slit according to the animals' performance and engagement. By the fifth day, the fourth position of the spacer was reached, corresponding to approximately 12 mm from the slit. In addition, it was observed that the central alignment of the tip relative to the slit was not optimal, as the animals were able to reach the water droplet with both forelimbs. This was undesirable since the camera was positioned to specifically capture movements of the right forelimb. This observation led to the adoption of Version 0.1 in the subsequent phase.

During the kinematic assessment phase, the droplet volume was reduced to 5 μl in an attempt to encourage the animals to perform more reaching movements. Although all mice exhibited natural reaching behaviour during the reaching phase, some individuals showed a marked decrease in performance. In such cases, the distance to the water droplet was adjusted by progressively moving the droplet closer to the slit. In addition, several changes were made to the illumination, the surroundings of the setup, and within the script itself to enable real-time monitoring of behavioural metrics. At the beginning of

week 2, the setup was upgraded to Version 0.1, and the structural hardware changes were associated with an improvement in the animals' engagement and with a more consistent use of the right forelimb during reaching.

3.3.2 Pilot experiment

3.3.2.1 Animals

A total of 24 mice (14 DYT and 10 WT littermate controls) were included in the pilot experiment, with their individual characteristics summarised in Table 3.2:

Table 3.2: Animal cohort details for the pilot experiment.

Mouse ID	Sex	Genotype	Surgical condition	Starting weight (g)	Age (weeks)
5176	♀	DYT	Viral Injection + Lens	20.4 ± 0.1	18
5177	♀	DYT	Viral Injection + Lens	21.6 ± 0.1	18
5212	♀	WT	EMG	22.3 ± 0.1	16
5242	♂	DYT	Viral Injection + Lens	27.6 ± 0.1	16
5256	♀	DYT	—	19.8 ± 0.1	15
5257	♀	WT	—	23.3 ± 0.1	15
5266	♂	DYT	EMG	26.6 ± 0.1	15
5267	♂	DYT	EMG	29.9 ± 0.1	15
5278	♂	DYT	Viral Injection + Lens	28.5 ± 0.1	14
5280	♂	DYT	Viral Injection + Lens	26.5 ± 0.1	14
5281	♂	WT	Viral Injection + Lens	28.0 ± 0.1	14
5282	♂	WT	Viral Injection + Lens	26.9 ± 0.1	14
5283	♀	DYT	Viral Injection + Lens	21.6 ± 0.1	14
5287	♀	WT	Viral Injection + Lens	21.5 ± 0.1	14
5291	♀	WT	Viral Injection + Lens	22.9 ± 0.1	14
5296	♂	DYT	—	30.9 ± 0.1	14
5316	♀	DYT	—	25.2 ± 0.1	14
5318	♀	WT	—	20.5 ± 0.1	14
5319	♀	DYT	EMG	19.6 ± 0.1	14
5327	♂	WT	—	25.6 ± 0.1	14
5329	♂	DYT	Viral Injection + Lens	26.5 ± 0.1	14
5330	♀	DYT	Viral Injection + Lens	20.6 ± 0.1	14
5334	♂	WT	EMG	25.0 ± 0.1	13
5335	♂	WT	EMG	26.0 ± 0.1	13

Note. Starting weight refers to experimental day 1 (*i.e.*, after water deprivation). Starting age indicates the number of full completed weeks at the beginning of the experimental protocol. WT – wild-type; DYT – heterozygous carrier of the DYT1 mutation; ♂ – Male; ♀ – Female; Viral Injection + Lens – Viral injection of AAV5.CAG.GCaMP6f and cranial window implantation (lens and baseplate); EMG – intramuscular electrode implantation for electromyographic recordings.

The mice were kept under the same conditions as described in Section 3.3.1.1, differing on the fact that during the experimental periods the amount of water was not capped, typically reaching around 1.0 ± 0.5 ml per day. The experiment was conducted five days per week and on non-experimental days, acidified water ($\tau_{C_6H_8O_7} = 0.02$) was provided *ad libitum* to maintain hydration without interfering with behavioural performance [53]. All the experiments were performed during the light part of the cycle, with approximately 24 hours between sessions.

In parallel, a study was conducted to investigate the relationship between muscle activity, neural

dynamics, and movement kinematics. To this end, 6 mice (3 DYT and 3 WT) were surgically implanted with intramuscular electrodes for EMG recordings in four areas of the forelimb: *triceps brachii (caput longum)*, *triceps brachii (caput laterale)*, *biceps brachii*, and *deltoideus (pars scapularis)*; additionally, 12 mice (8 DYT and 4 WT) were implanted with cranial windows and injected with a viral vector (AAV5.CAG.GCaMP6f) to enable D1 neuron fluorescence for *in vivo* calcium imaging.

All surgical procedures were performed two weeks before the start of the experimental protocol and carried out in accordance with the protocols described by Chung, *et al.* [54] and Mendonça, *et al.* [55], respectively. EMG and imaging recordings were performed twice per week to reduce experimental burden, and on days without recordings, dummy implants matching the size and weight of the original hardware were placed to ensure consistent loading and habituation across all sessions.

3.3.2.2 Protocol

This experimental phase aimed to validate the final individual version of the reaching chamber and ensure that it was ready to be adapted to a home-cage environment.

The experiment was conducted over a seven-week period (Figure 3.8), beginning with an extended initial phase of training and habituation, followed by kinematic assessment across five consecutive weeks.

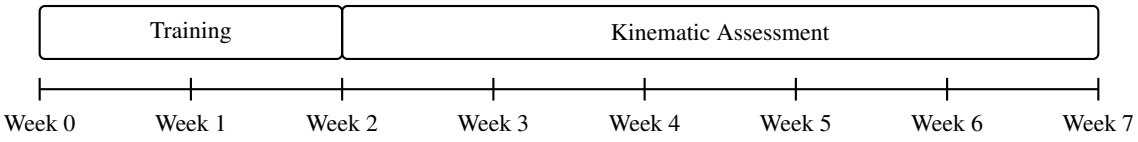

Figure 3.8: Schematic representation of the pilot experimental timeline.

Each session lasted 30 minutes per animal, with no maximum daily water intake enforced. Two chambers were used in parallel, one dedicated to males and the other to females, ensuring that only one gender was ever housed per box, as smell and the awareness of the presence of the opposite gender can affect behaviour [56]. Version 0.5 of the setup was used throughout the experiment, and the software was automated following the protocols described in Sections 3.1.2.1-3.1.2.4.

During the training phase, 5 μl water droplets were delivered to the animals, and the tip was gradually positioned further from the slit according to the animals' performance and engagement. The final tip position was selected based on the maximum distance that the animal could consistently reach without difficulty. This position was determined iteratively and based on experimenter's observation, adjusting the distance until the animal performed several consecutive reaches reliably.

During the kinematic assessment phase, 5 μl droplets continued to be used, and the animals were placed in the chamber without any disturbances, allowing them to perform RtG movements freely as many times as they wished. In very rare cases where a mouse failed to perform reaches for two consecutive days, the tip distance was slightly adjusted to recover the animal's performance (occurred in only 2 out of the 24 animals across the 7 weeks).

In parallel to the kinematic assessment, EMG signals were recorded twice per week to characterise muscle activity during RtG execution and regarding the *in vivo* calcium imaging, data collection was scheduled across the week considering the available hardware and to avoid overloading of the animals: six females were measured on Mondays and Thursdays, while six males were measured on Tuesdays and Fridays.

After the main experiment, an exploratory phase took place, during which systematic variations in tip position were introduced to test whether the animals would continue to perform the task when faced

with altered reach demands. Four animals were tested under these conditions, with their performance and behavioural adaptations observed qualitatively.

3.3.3 24-hour experiment

3.3.3.1 Animals

A total of 6 mice were included in the 24-hour experiment, comprising two subgroups, each following its own protocol, based on surgical conditions: three WT mice without any implant, and three mice implanted with RFID tags, including one DYT and two WT. Their individual characteristics are summarised in Table 3.3:

Table 3.3: Animal cohort details for the 24-hour experiment

Mouse ID	Sex	Genotype	Surgical condition	Starting weight (g)	Age (weeks)
5835	♂	WT	—	28.6 ± 0.1	12
5836	♂	WT	—	28.4 ± 0.1	12
5839	♂	WT	—	30.6 ± 0.1	12
5806	♂	WT	RFID Implant	29.7 ± 0.1	17
5809	♂	DYT	RFID Implant	31.9 ± 0.1	17
5810	♂	WT	RFID Implant	30.9 ± 0.1	17

Note. Starting weight refers to experimental day 1 (*i.e.*, after water deprivation). Experimental day 1 is different for the two subgroups. Starting age indicates the number of full completed weeks at the beginning of the experimental protocol. WT – wild-type; DYT – heterozygous carrier of the DYT1 mutation; ♂ – Male; ♀ – Female.

In this experiment, the goal was to habituate the mice to remain inside the setup 24 hours a day, moving freely between the home-cage and the reaching chamber. To this end, the protocol distinguishes between phases in which the animals performed daily sessions and those in which they were kept permanently in the setup.

When daily sessions were performed, the mice were kept under the same conditions as described in Section 3.3.2.1 and typically consumed on average 2.5 ± 1.5 ml of water per day. In Protocol 1, the experiment was conducted over eight days, with a two-day interval between the first three and the last five days. In Protocol 2, the experiment was conducted over seven days, with a two-day interval between the first two and the last five days. On non-experimental days, acidified water ($\tau_{C_6H_8O_7} = 0.02$) was provided *ad libitum* to maintain hydration without interfering with behavioural performance [53]. All the daily sessions were performed during the light part of the cycle, with approximately 24 hours between sessions.

The RFID tags were implanted through a minor surgical procedure and placed subcutaneously between the scapulae, slightly below the neck. For the implantation, the mice were anaesthetised with isoflurane, using 4.0% for induction and 1.0% for maintenance, delivered in oxygen at a flow rate of 1.0 L/min.

3.3.3.2 Protocol 1

This protocol, illustrated in Figure 3.9, used animals from the first subgroup and was intended to be applied until the setup allowed continuous 24-hour operation. The final version of the reaching chamber (Version 0.5), was used, with the door from Version 1.0 connecting it to the home-cage. Regarding the software, all protocols described in Sections 3.1.2.1–3.1.2.4 were followed. The door system protocol

described in Section 3.1.2.6 was intended to be implemented during Week 1 but this phase was not reached, therefore, the door control was fully manual.

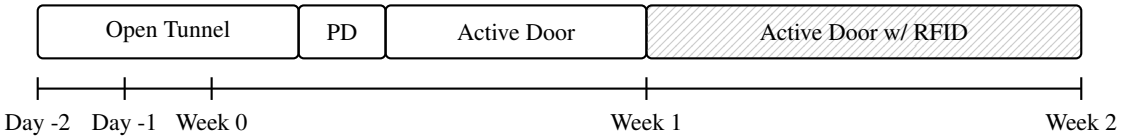

Figure 3.9: Schematic representation of the first protocol for the 24-hour experimental timeline. PD – Passive door.

On the first day of the experiment, the mice were placed individually in the home-cage for 3 hours with the open tunnel connecting to the reaching chamber for three hours. Due to time constraints and having only one setup available, only two animals could be tested on the first day, and the third was placed on the following day. On this second day, the remaining animals did not perform sessions, and 1 μl of water was provided to them.

On the third and fourth days of the experiment, all three animals were placed together in the home-cage for three hours, still with the open tunnel connecting to the reaching chamber and no intervention from the experimenter occurred.

On the fifth day, another three-hour session was conducted during which a passive rotary door was implemented, allowing the animals to push it to move between compartments and habituating them to its presence. Additionally, halfway through the session an external motor was manually operated to simulate the sound later produced by the servo when activating the door mechanism, aiming to familiarise the mice with this future auditory cue.

On the sixth day, the active servo-driven rotary door was implemented, with the mechanism manually activated by the experimenter. When a mouse fully entered a compartment, the door rotated around its axis to allow passage between the home-cage and the reaching chamber, and vice versa.

During the seventh and eighth days, the same system was maintained under experimenter control. Following these sessions, a decision was made to interrupt the experiment before transitioning to RFID-controlled access, as discussed in Chapter 4.

3.3.3.3 Protocol 2

This protocol, illustrated in Figure 3.10 used animals from the second subgroup with the same objective of keeping them for 24 hours in the setup, free to alternate between the home-cage and the reaching chamber. The final version of the reaching chamber (Version 0.5), was used, with the door from Version 1.1 connecting it to the home-cage. Regarding the software, the protocols for session initialisation, water delivery, and video capture, as described in Sections 3.1.2.1–3.1.2.4, were followed throughout the experiment, while the protocols for animal identification and the RFID stopper system, described in Sections 3.1.2.5 and 3.1.2.7, were tested and implemented progressively.

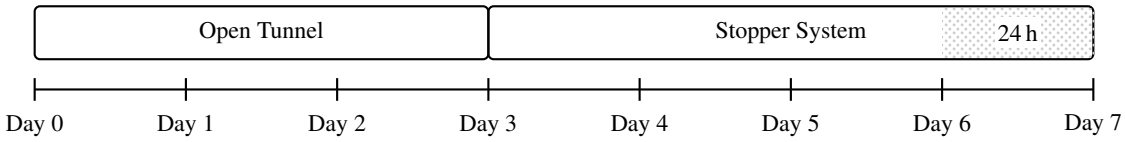

Figure 3.10: Schematic representation of the second protocol for the 24-hour experimental timeline.

On the first day, all animals were placed individually in the home-cage for two hours, with the open tunnel left accessible to allow each mouse to explore the environment and habituate to the setup.

On the second day, all animals were placed together in the same environment for four hours, with the open tunnel remaining in place, providing them with the opportunity to interact and gradually become familiar with each other within the shared space.

On the third day, the same procedure was performed, placing all mice together with the open tunnel connecting the home-cage and the reaching chamber. The animals were removed after three hours and thirty minutes as they had been sleeping for the last thirty minutes.

On the fourth and fifth days, we transitioned to a manually controlled stopper system, placing all animals together for a four-hour session. Whenever an animal moved from one side to the other, the experimenter rotated the servo to allow it to push the door and enter the reaching chamber, simultaneously preventing the other animals from passing, and vice versa. On the fifth day, the protocol for identifying the animals using RFID was implemented, as described in Section 3.1.2.5.

On the sixth day, the animals were placed together and the RFID stopper system functioned automatically, without experimenter intervention, as described in section 3.1.2.7. The animals were supervised for six hours and, since no issues occurred, they were left overnight until the seventh day, remaining in the setup for a total of 29 hours. To ensure that no problems arose, a video system and remote connection to the computer were also installed to monitor the animals and metrics in real time.

Chapter 4

Experimental Results

In this chapter, we present the results of the experimental procedures carried out in this dissertation and provide a comprehensive discussion of their implications. These experiments were designed to troubleshoot technical challenges encountered during the development of the setup and to validate its functionality. The choice of experimental parameters and the selection of tests were informed not only by evidence from the literature but also by prior work conducted within the scope of this dissertation and by previous experiments performed in the laboratory.

4.1 Early-prototype experiment

This experiment represented the first implementation of the reaching chamber and aimed to assess the basic feasibility of the task under partially automated conditions. Both video acquisition and water reward delivery were automated, allowing the collection of short behavioural clips, illustrated in Figure 4.1, without direct human interference.

Figure 4.1: Samples of video frames illustrating the different phases of a reach-to-grasp movement collected during the early-prototype experiment.

Due to ongoing refinements in experimental conditions and hardware, the application of MT techniques was not feasible at this stage. Consequently, our analysis focused on parameters that may serve as proxy indicators of animal performance, such as the number of pump activations and the number of recorded clips (Figure 4.2).

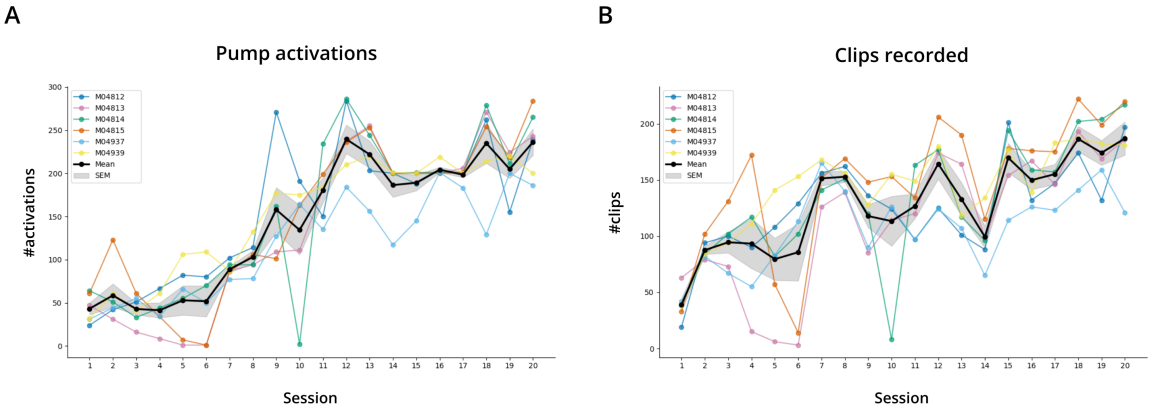

Figure 4.2: Number of pump activations (A) and clips recorded (B) per animal across sessions in the early-prototype experiment.

We observed a gradual increase in both metrics, which began to stabilise towards the end of Week 1 (around session 10). A sharper rise was noticeable in the transition from Week 0 to Week 1, most likely associated with the reduction in droplet volume starting on session 6 (from 10 μl to 5 μl).

At this stage, the number of reaching attempts performed by each animal was not directly recorded. Nevertheless, both metrics provide reasonable approximations. Pump activations correspond to successful reaches in which the animal accessed and removed the droplet from the tip, while the number of recorded clips represents the minimum number of reaching attempts, since each clip is triggered by a reach and separated from the next by at least three seconds.

While no marked differences were detected between individual animals, we also examined potential differences when grouping them by genotype. Figure 4.3 illustrates this exploratory analysis, although no conclusive genotype effect was observed.

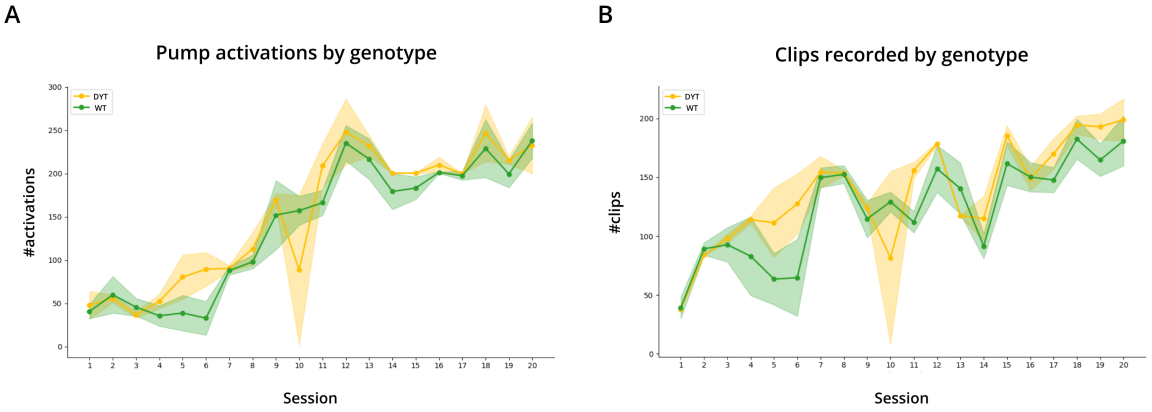

Figure 4.3: Number of pump activations (A) and clips recorded (B) by genotype across sessions in the early-prototype experiment.

Additionally, we sought to assess the animals' performance throughout each session. To this end, we based our analysis on the metric of pump activations, examining how these varied over time with respect to activations per minute. This is illustrated in Figure 4.4:

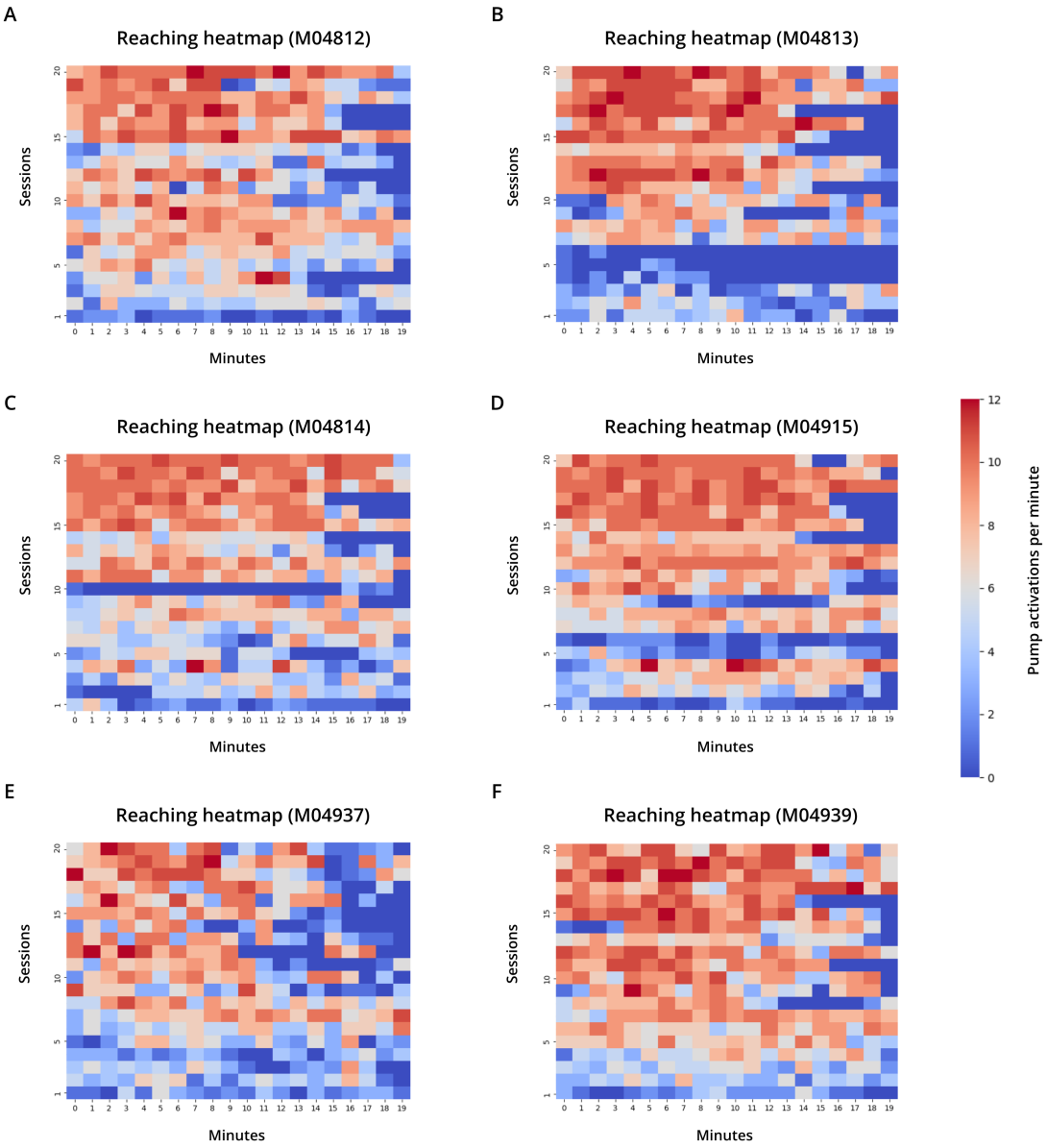

Figure 4.4: Heatmaps illustrating the temporal distribution of pump activations for individual animals, as indicated in each plot title. Each row represents a single session, while the colour intensity reflects the frequency of pump activations per minute.

When analysing the heatmaps, we observed that the number of pump activations, which serves as a proxy for successful reaching attempts, increased progressively across sessions, indicating that the animals were gradually learning the task.

From session 10 onwards, once the animals were considered habituated, the intra-session activity profile showed a distinct temporal pattern: the highest frequency of pump activations was concentrated at the onset of the session, followed by a marked decline in activity during the final five minutes. This suggests that the animals rapidly engaged with the task upon session initiation, with motivation or engagement decreasing as the session progressed, potentially reflecting satiety.

This early phase informed key design decisions and prepared the foundation for the subsequent pilot experiment, where chamber geometry and behavioural readout were further optimised.

4.2 Pilot experiment

This experiment aimed to establish a final version of the reaching chamber that could later be connected to a home-cage environment. Beyond the development of the chamber itself, this stage also served to validate the full analysis pipeline described in Section 3.2, confirming its suitability for extracting reliable kinematic parameters. Furthermore, it provided an opportunity to test the feasibility of incorporating external wired measurements, including EMG and *in vivo* calcium imaging, in parallel with the behavioural recordings, thereby evaluating the chamber's compatibility with multimodal experimental approaches. The EMG analysis was carried out by Simon Zamora (Champalimaud Foundation), while the *in vivo* calcium imaging analysis was performed with the help of Pedro Dias (Champalimaud Foundation).

Here, we obtained clips of greater reliability and consistency compared to those collected during the early-prototype experiment, providing stable datasets across sessions. This ensured that the data could be reliably analysed using DLC. An illustrative example is shown in Figure 4.5:

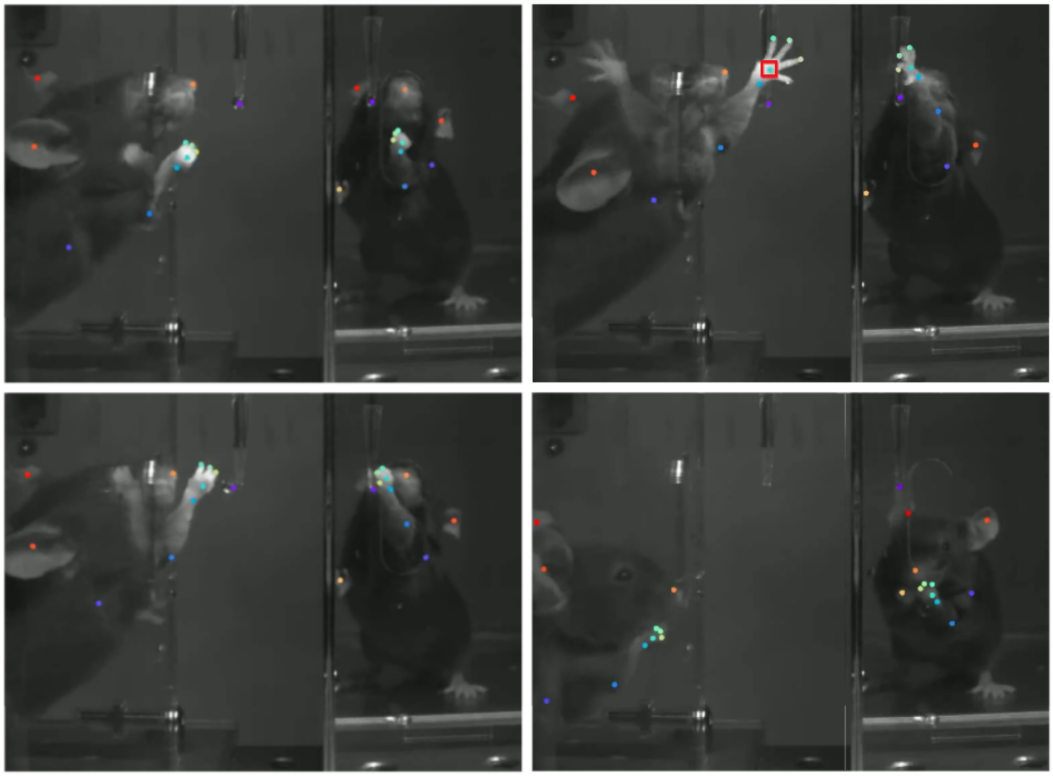

Figure 4.5: Samples of video frames illustrating the different phases of a reach-to-grasp movement collected during the pilot experiment. Colored dots in the frames denote the anatomical landmarks of the forelimb that were estimated using DLC.

In Figure 4.5, the 12 keypoints described in Section 3.2.2 are illustrated across a representative reaching movement. For the kinematic analysis, we restricted our focus to the trajectory of the centre of the right paw, highlighted with a red square. Only the lateral view of the reach was considered to streamline the analysis, since the frontal perspective contributed minimal additional information for most kinematic metrics.

Data from Week 2 and Week 5 (1381 and 1591 clips, respectively) were considered, in order to compare movement trajectories at two distinct experimental stages. Week 2 reflects an early period of stable task engagement, while Week 5 provides a later time point for assessing potential changes in

kinematic features. Note that mouse 5282 was sacrificed in Week 4 due to detachment of the implanted cap and was therefore excluded from all analyses.

The exclusion criteria described in Section 3.2.3 were applied, resulting in a total of 2123 clips, and the obtained trajectories are illustrated in Figure 4.6:

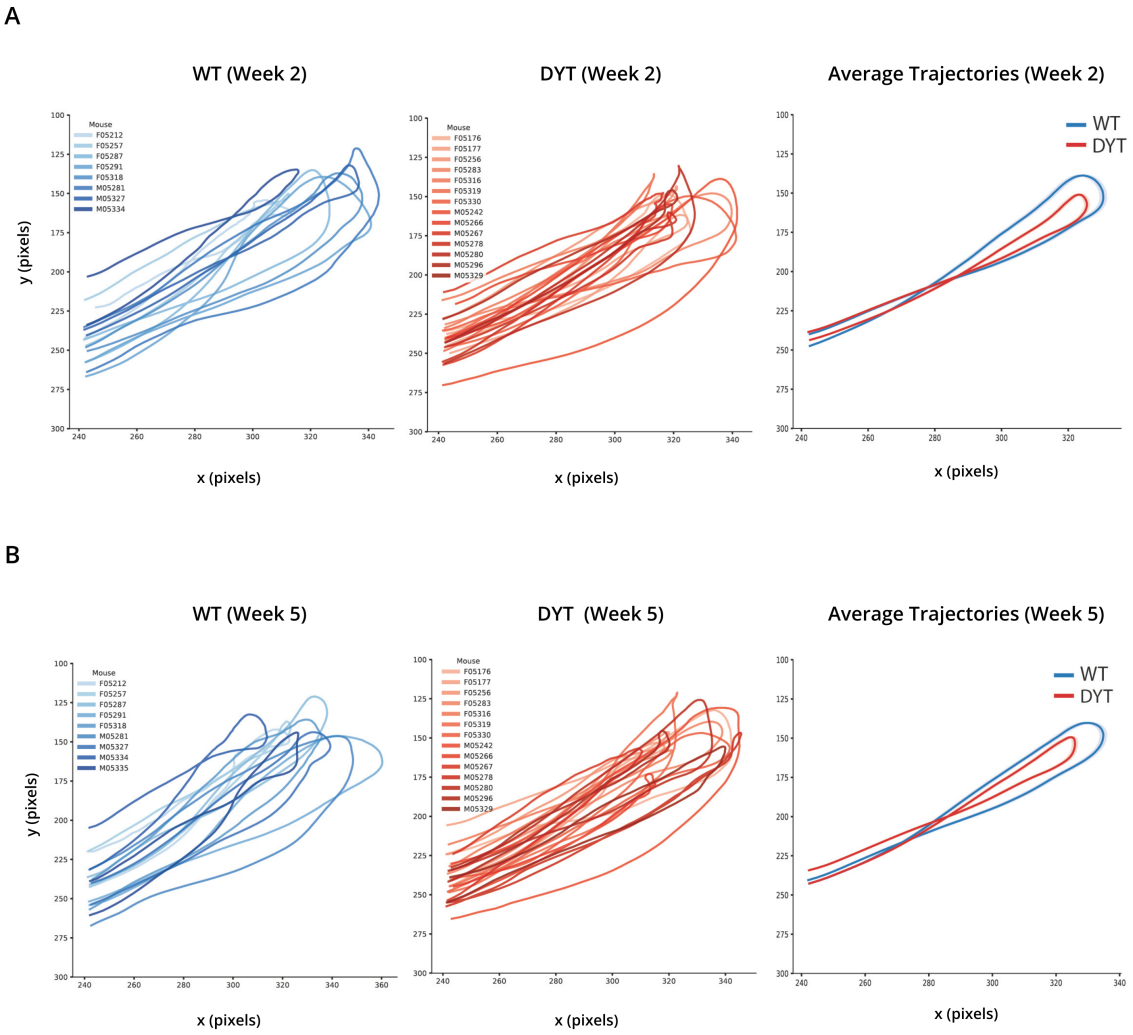

Figure 4.6: Average trajectories of reach-to-grasp movements at Week 2 and Week 5. Left – Average trajectories of the RtG movements performed by different WT mice (in blue) at Week 2 (A) and Week 5 (B) of the experimental protocol. Middle – Average trajectories of the RtG performed by different DYT mice (in red) at Week 2 (A) and Week 5 (B) of the experimental protocol. Right – Average trajectories of the RtG movements performed by group. The letter preceding each mouse ID denotes the sex of the animal (M – male, F – female). 100 pixels correspond to 15 mm. Sample sizes: W2, WT: n=8, DYT: n=14; W5, WT: n=9, DYT: n=14. Mouse 5335 did not perform any reach in Week 2.

While there is substantial variability within each group, WT animals exhibit a greater reach extent, often extending beyond the droplet position. Since each individual animal had a slightly different distance to the droplet, despite the average droplet distance being consistent across groups (approximately 15 mm), analyses based solely on raw trajectories may not fully capture differences in performance or reach scaling (see Appendix E for details regarding the droplet distance).

To further characterise the dynamics of the movements, the raw trajectories were differentiated with respect to time, from which velocity and acceleration profiles were obtained. Since the RtG movements were not subdivided into reaching and retrieving phases, the sign of the curves indicates the direction of movement: positive values correspond to the reaching phase, whereas negative values correspond to the

retrieving phase. These profiles are shown in Figure 4.7:

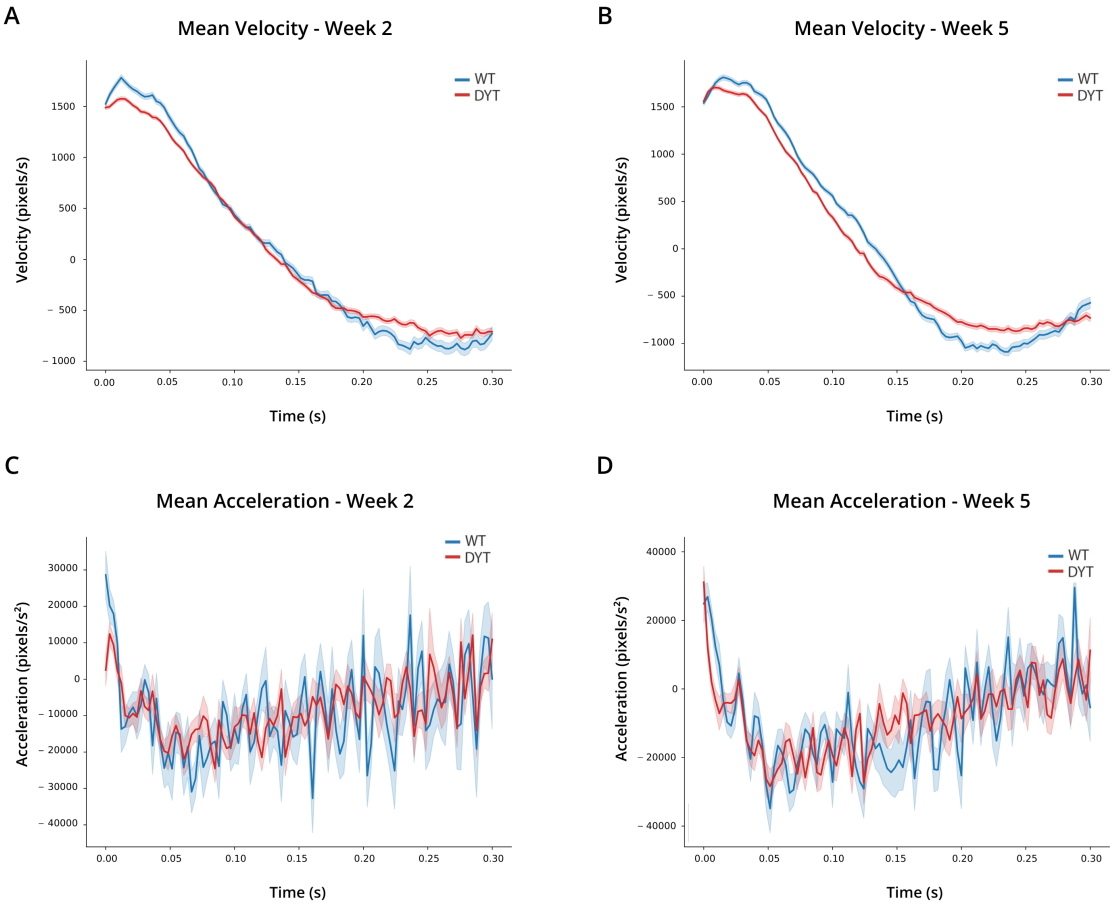

Figure 4.7: Velocity and acceleration profiles of the reach-to-grasp movements. A – Mean velocity profiles of the trajectories recorded at Week 2. B – Mean velocity profiles of the trajectories recorded at Week 5. C – Mean acceleration profiles of the trajectories recorded at Week 2. D – Mean acceleration profiles of the trajectories recorded at Week 5.

By analysing Figure 4.7, the absolute differences in velocity profiles appear more pronounced at Week 5, potentially indicating group-specific motor adaptation. As noted previously for the trajectories, the RtG movement exhibits considerable inter-animal variability, which introduces substantial noise into the data and complicates the identification of consistent group-level patterns. This variability needs to be taken into account when interpreting the kinematic metrics and highlights the importance of normalisation and complementary analyses.

To account for individual differences in the droplet position, the trajectories were subsequently normalised relative to the distance from the slit to the tip. Under this normalisation, one unit corresponds to the Euclidean distance between the slit and the droplet position for each animal. Consequently, an optimal movement would yield a total distance of 2 units: one unit for the reaching trajectory and one unit for the retrieving.

In Figure 4.8, we present the key metrics analysed in this study, including those described in Section 3.2.3: total distance, mean velocity, peak velocity, time to peak velocity, mean acceleration, peak acceleration, movement smoothness, path efficiency, reaching time, initial direction error, and endpoint variability. All metrics were computed after normalisation and are presented as genotype comparisons.

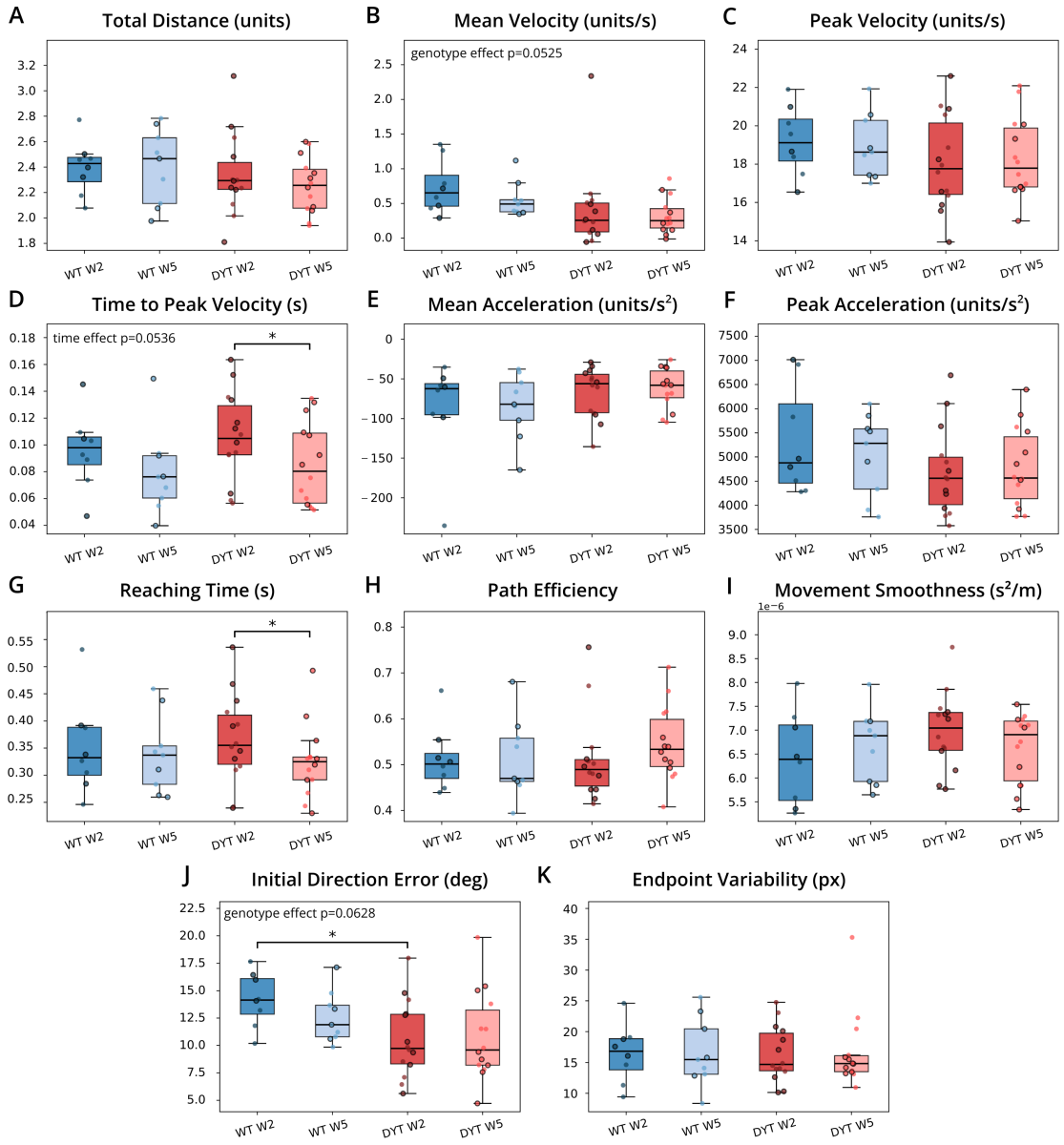

Figure 4.8: Temporal kinematic metrics of reach-to-grasp movements. Box plots depict kinematic parameters of WT and DYT mice at Week 2 (W2) and Week 5 (W5) of the pilot experiment. A – Total distance. B – Mean velocity. C – Peak velocity. D – Time to peak velocity. E – Mean acceleration. F – Peak acceleration. G – Reaching time, representing the duration for a mouse to complete a full reach-to-grasp movement. H – Path efficiency, quantifying the straightness of the trajectory. I – Movement smoothness, calculated as the inverse of mean absolute acceleration, reflecting motion fluidity. J – Initial direction error, quantifying the angular deviation from the ideal path at movement onset. K – Endpoint variability, representing the dispersion of the final paw position (on the closest point to the droplet). Statistical significance was tested using a mixed-effect model analysis, * dentoes p-value < 0.05. Each point represents the mean of all reach-to-grasp movements performed by a mouse in the considered session. Data points with an outline indicate male animals, whereas those without an outline represent females. Sample sizes: W2, WT: n=8, DYT: n=14; W5, WT: n=9, DYT: n=14. Mouse 5335 did not perform any reach in Week 2.

Analysing Figure 4.8, the distance profiles indicate that both groups converge around 2.4 units, with no evident change over time. Regarding mean velocity, WT animals consistently exhibited a trend towards higher values compared to DYT at both timepoints, with a main effect of genotype approaching significance ($p = 0.0525$). In contrast, peak velocity remained similar across groups. For time to peak velocity, both genotypes displayed a decreasing trend across weeks. A main effect of time was observed ($p = 0.0536$), with DYT animals showing a statistically significant reduction, whereas WT animals did

not, most likely due to limited statistical power. No substantial differences were found in mean or peak acceleration, which is consistent with the relatively similar profiles observed in Figure 4.7.

Regarding reaching time, values fluctuate around 0.3 seconds across all subgroups, which motivated limiting the time axis in Figure 4.7 to this range, and we observed a significant decrease in DYT animals. For path efficiency and movement smoothness, no significant differences were detected. Concerning initial direction error, DYT animals exhibited lower errors compared with WT, with a significant difference at Week 2. Additionally, although not statistically significant, WT animals showed a decreasing trend in error across weeks, whereas DYT animals remained stable, suggesting a potential lack of learning or adaptation over time. This apparent plateau could also reflect a floor effect, where performance is already near the lower limit of measurable error. No differences were observed in endpoint variability between groups.

Although insights can be extracted from comparing groups across weeks, it is important to consider the inherent variability of the RtG task. Individual animals often display distinct motor strategies when performing the movement, meaning that differences observed at the group level may not necessarily reflect systematic adaptations but rather natural inter-animal variability.

Additionally, we assessed chronic EMG in a subset of animals (3 WT and 3 DYT) to evaluate muscle physiology, which is highly relevant to assessing muscle co-contraction (a feature of dystonia). Although these data were only explored at a preliminary stage, motor unit action potentials could be identified, as illustrated in Figure 4.9. Such recordings may serve in future analyses to characterise putative differences in muscle synchronicity between DYT and WT mice across sessions.

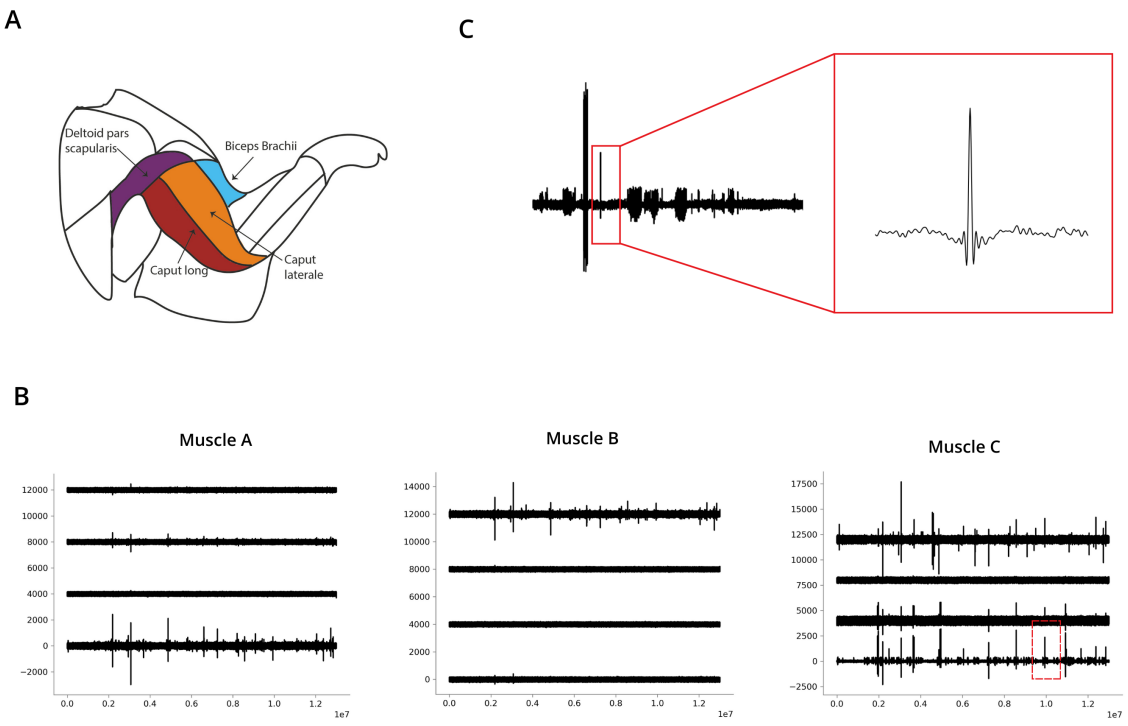

Figure 4.9: Electromyography of the forelimb muscles during RtG movements. A – Anatomical representation of the muscles where the high-density electromyography (“myomatrix”) arrays were implanted. B – Example recording showing the activity profiles of three of these muscles. C – Zoom of part of the recording in B, exhibiting a motor unit action potential (inset).

4. EXPERIMENTAL RESULTS

Following the verification that EMG recordings could be successfully performed under the experimental setup, we conducted an initial exploratory assessment of *in vivo* calcium imaging, as illustrated in Figure 4.10, to evaluate the compatibility of the reaching chamber with wired neural recordings.

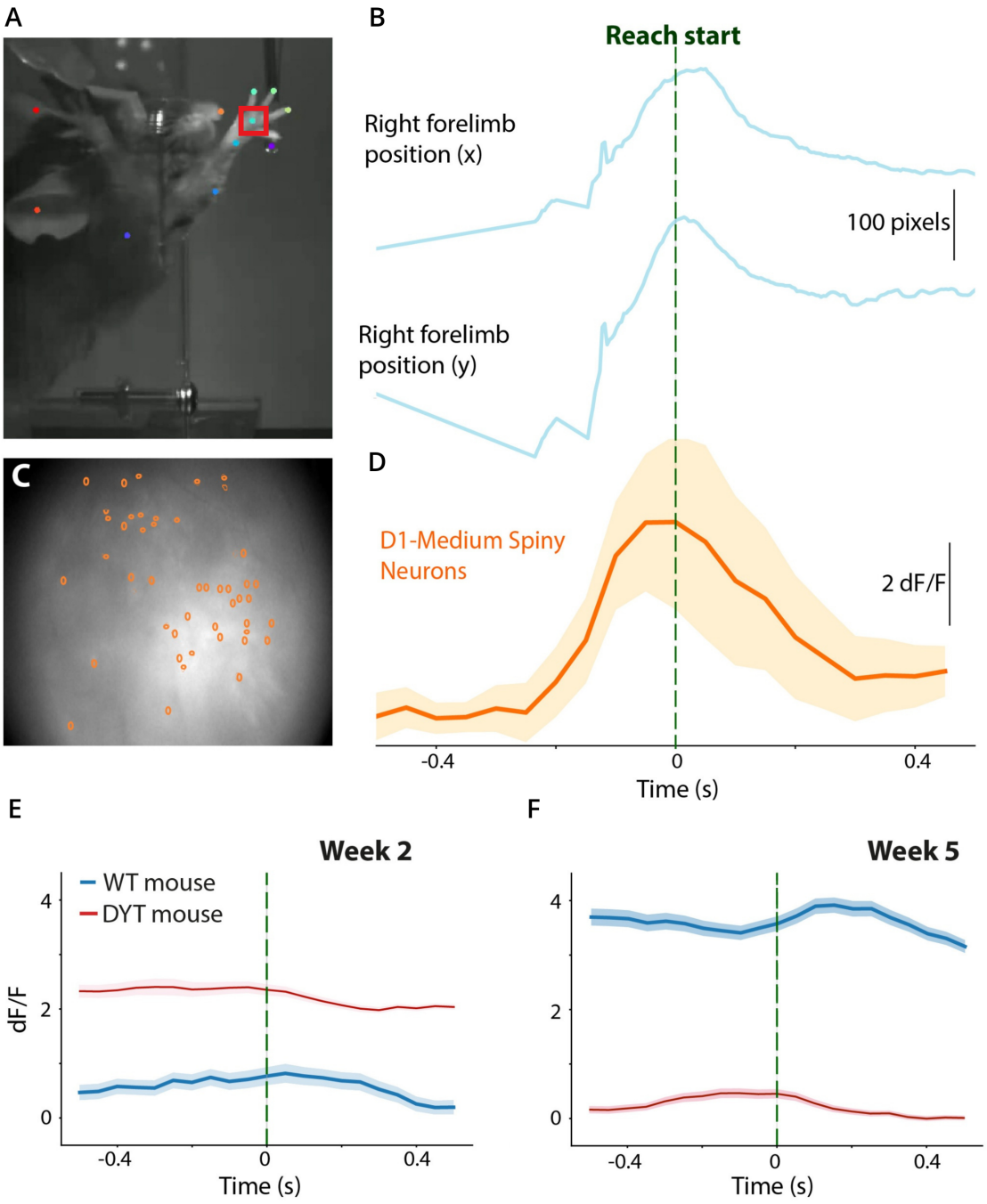

Figure 4.10: *In vivo* calcium imaging of D1-medium spiny neurons (MSNs) during reach-to-grasp movements. A – The centre of the right paw (highlighted by the red square) was used to track the B – forelimb position and define the start of each reach-to-grasp movement, represented with a dotted green line. C – Image of an example field of view of the dorsolateral striatum with the detected D1-MSNs (orange circles) and D – their corresponding mean of the difference in fluorescence, aligned to reach start. Mean difference in fluorescence activity of the D1-MSNs of an example WT mouse (in blue) and one DYT mouse (in red) at Week 2 (E) and Week 5 (F) of the protocol. Neural activity data are presented as mean ± SEM.

Here, we show as an example the spatial location and temporal dynamics of neurons from 1-photon calcium imaging movies of a single mouse. By aligning neuronal activity to movement onset, this approach will allow the comparison of D1-MSNs activity between DYT and WT mice during RtG movements, as well as across sessions, thereby providing insight into the correlation between activity and the potential development of an overuse phenotype (as shown in Figure 4.10 – E,F).

Following the completion of the previous experimental phase, an exploratory protocol was implemented to assess reach adaptability. In this protocol, the servo-controlled spout was alternated between higher and lower positions relative to the slit opening, requiring the animals to adjust their forelimb trajectories to reach the water. Only four animals were used for this assessment, and their performance is summarised in Appendix D.

It was observed that the animals can adapt their reaching movements to different spout heights with varying difficulty, allowing future experiments to explore a range of positions depending on the specific objectives.

4.3 24-hour experiment

In this experiment, our objective was to connect the reaching chamber to the home-cage in a configuration that allowed animals to move freely between the two compartments, while ensuring individual access and proper identification. To this end, two protocols were tested, as described in Section 3.3.3.

No kinematic analysis was conducted here, as the primary aim was the validation of the developed system. The following section therefore presents a longitudinal assessment across consecutive training stages, focusing on performance-related metrics such as the number of reaching attempts and crossings between compartments, complemented by an observational characterisation of animal behaviour.

4.3.1 Protocol 1

4.3.1.1 Open tunnel

During the first habituation session, animals were placed individually in the home-cage connected to the reaching chamber via an empty tunnel, allowing initial exploration. Mouse 5839 remained in the home-cage for approximately one hour before approaching the tunnel. At around 1h45min, it entered the reaching chamber for the first time and shortly thereafter interacted with a water droplet, first licking it and then performing reaching movements. Over the 3-hour session, the animal crossed the tunnel more than 20 times, although its overall exploratory behaviour remained moderate.

In contrast, mouse 5835 crossed the tunnel and entered the reaching chamber within the first 3 minutes. It explored the chamber for about 5 minutes before becoming aware of the water droplet around minute 20, at which point it initiated licking behaviour. Despite this interaction, the animal did not return to the droplet for almost 50 minutes. At approximately 1h20min, it showed signs of inactivity and fell asleep until the end of the session.

Mouse 5836 immediately discovered the tunnel upon placement in the home-cage and began actively exploring it. Within 10 minutes, it licked the water droplet and subsequently attempted a small number of reaching movements. Throughout the session, it exhibited pronounced exploratory behaviour, crossing the tunnel more than 50 times. Nevertheless, consistent reaching was not observed, most likely due to low motivational drive, as the animal often showed disinterest after consuming a single droplet.

After the individual sessions, three mice were tested simultaneously. On the third day all animals explored the tunnel and reaching chamber without difficulty, suggesting rapid habituation to the setup.

Occasional social interactions were noted, as well as some stress-related behaviours such as digging. All animals licked the water droplet and attempted reaching movements. Two mice fell asleep after approximately 2h20min but re-engaged later in the session. Mouse 5835 displayed particularly high engagement, performing more than 100 reaching movements.

On the fourth day robust engagement with the system was observed. In the first 30 minutes alone, more than 250 reaching movements were recorded. While animals typically entered the reaching chamber individually, episodes of simultaneous access and competition for the water were observed. Over the 3-hour session, a total of 1,135 water droplets were automatically dispensed, corresponding to 2,283 reaching attempts across all animals. On average, each mouse performed 761 reaching attempts and consumed 378 droplets.

4.3.1.2 Passive door

A passive door system was introduced on the fifth day, requiring animals to push the door to move between compartments. Mouse 5836 was the first to cross the door and performed 210 reaches within the first 10 minutes. The second mouse crossed at 20 minutes and executed 80 reaching movements during its initial attempt. The third mouse crossed at 35 minutes and performed 30 reaches. Across the full 3-hour session, the three mice completed a total of 2,527 reaching movements, with 1,013 droplets dispensed. This corresponds to an average of 843 reaching movements and 338 droplets per animal. Although engagement levels were high, the absence of any locking or controlled mechanism in the door meant that animals could push it open even when others were already inside the reaching chamber. This occasionally led to disturbances and interference between individuals, highlighting the need for a system capable of selectively blocking entry to ensure undisturbed task performance.

Additionally, from the midpoint of the session, a motor was manually activated to habituate the mice to the noise created by the future mechanisms and avoid a fear response in subsequent sessions. This manipulation did not noticeably affect the animals' behaviour or task performance, suggesting that the auditory cue alone did not disrupt exploration or reaching activity.

This arrangement worked well for habituation, promoting exploration and repeated door crossings, and based on this positive outcome we proceeded to implement the active door system.

4.3.1.3 Active door

On the sixth day, the active door system was introduced, with the mechanism manually activated by the experimenter. Mouse 5836 entered the reaching chamber after 3 minutes, performing 40 reaching movements and receiving 15 droplets. Mouse 5839 entered at 7 minutes, completing 38 reaches with 18 droplets. Mouse 5835 did not cross the mechanism at any point. Across the session, only 5836 engaged consistently with the reaching task, entering and exiting the chamber four times. The other two animals received supplementary water to maintain hydration while ensuring motivation for future sessions.

Using the same active door protocol, only mouse 5839 crossed the tunnel on the seventh day, doing so once during the entire session. Inside the reaching chamber, it performed 384 reaching movements and consumed 119 droplets. Due to low overall activity, the session was extended by 30 minutes, but no additional crossings occurred.

On the following day, the same protocol was used and only mouse 5836 crossed the tunnel, also performing a single entry. It completed 377 reaching movements and consumed 203 droplets. The other animals did not engage with the door and were therefore provided with supplementary water to meet hydration requirements.

Given the limited engagement observed across consecutive sessions, the protocol was ultimately discontinued. Although the animals occasionally interacted with the door, it became apparent that they developed an aversion to the active door system, likely due to the lack of control over when the door was opened. This reduced voluntary exploration and task engagement, indicating that the current implementation of the active mechanism was not well tolerated by the mice. In light of these observations, alternative door configurations, as described in Protocol 2, were subsequently explored.

4.3.2 Protocol 2

The second protocol aimed to allow animals from the second subgroup to freely alternate between the home-cage and the reaching chamber over extended periods, building on the insights gained from the previous experiment.

4.3.2.1 Open tunnel

During the initial habituation session, animals were placed individually in the home-cage with an open tunnel, allowing unrestricted exploration of the environment. All three mice quickly engaged with the tunnel and the reaching chamber, crossing the tunnel multiple times and interacting with the water droplets. Reaching behaviour was observed shortly after initial droplet interaction, with individual counts ranging from approximately 200 to 270 attempts over the session, demonstrating rapid familiarisation with the setup.

On the following day, animals were placed together in the setup. Immediate engagement with the reaching task was observed, with a high number of crossing events and reaching attempts during the first 30 minutes (approximately 500 reaches and 350 dispensed droplets, corresponding to ~ 16.7 reaches/min). However, reaching activity decreased significantly over subsequent intervals, dropping by approximately 81% during the last 90 minutes of the session, despite continued exploratory behaviour such as grooming and tunnel crossings. This pattern of high initial engagement followed by gradual decline was consistently observed in subsequent multi-animal sessions.

During the third day, immediate engagement with the reaching chamber was again observed. Intense competition for water occurred, particularly between 5806 and 5809, with repeated interactions indicative of social hierarchy dynamics. Each mouse received over 300 water droplets during the session and reaching activity progressively declined across intervals: after the first 30 minutes, 950 reaches were recorded; the following 30-minute interval contributed an additional 409 reaches (13.6 reaches/min, -57% relative to the first interval); the third hour added 274 reaches (4.6 reaches/min, -66% relative to the previous interval); and the final hour accounted for 97 reaches (1.6 reaches/min, -65% relative to the previous hour, -95% relative to the first 30 minutes).

4.3.2.2 Stopper system

With the implementation of the manually controlled stopper system on Days 4 and 5, animals successfully learned to operate the mechanism to access the reaching chamber individually, while preventing simultaneous passage by other mice. Reaching performance remained high, with cumulative counts per session reaching several hundred attempts per animal and droplet dispensation closely tracking task engagement. Importantly, the introduction of the stopper system did not adversely affect exploratory behaviour or overall task performance. In addition, the identification protocol described in Section 3.1.2.5

was implemented, allowing both video clips and performance metrics to be automatically stored and associated with the specific animal entering the reaching chamber.

With individual identification successfully implemented, the automatic RFID-controlled stopper system was introduced for extended 24-hour sessions on Days 6 and 7. Animals were able to freely alternate between compartments. After confirming stable operation during an initial 6-hour monitoring period, they were left overnight until the seventh day, remaining in the setup for a total of 29 hours. Reaching attempts and droplet dispensation were consistently recorded throughout, demonstrating sustained task engagement. Across the 29 hours of continuous activity, mice performed several thousand reaching movements (4,776 in total), indicating that the setup reliably supported uninterrupted task performance without adverse effects. Furthermore, activity was balanced across the three animals and showed a marked increase during the dark phase of the light–dark cycle, with a +24% increase in reaching relative to the light phase when considering the first 24 hours.

Overall, the results of Protocol 2 confirm that the combination of an open tunnel, stopper system, and RFID-based identification allows mice to self-initiate reaching movements in a socially housed environment, while preserving individual task metrics and avoiding interference from group dynamics. These findings validate the feasibility of long-term, minimally supervised behavioural assessment in the home-cage context.

Chapter 5

Proposed Protocol

Building upon the different iterations and experiments conducted to validate the behavioural setup, this chapter outlines a proposed protocol that consolidates the key elements considered essential for its correct and reproducible operation.

5.1 Setup requirements

In designing the reaching chamber, several requirements must be satisfied to ensure consistent and reproducible execution of the task. One requirement is that the aperture must allow a full forelimb extension so that animals can perform the complete reach-to-grasp movement. To meet this, the slit was dimensioned to permit the extension of the paw while restricting other body parts. Another requirement was that animals should use the right paw. This was achieved by placing the water spout off-centre, with the geometry of the task naturally guiding the animal toward right forelimb use. A further requirement is that the configuration must support progressive training and potential adjustments. For this purpose, the spout position can be adjusted to vary the distance to the reward, shaping performance across sessions. Finally, animal welfare must be preserved, which was ensured by designing the chamber so that the task can be executed without unnecessary discomfort or stress.

Illumination and recording also impose specific requirements. Constant and reliable lighting must be maintained across the full duration of the session. To achieve this, an infrared spotlight was used, providing stable illumination regardless of light or dark phases. Additionally, accurate motion capture is essential, which was ensured by the integration of a high-speed camera capable of recording with sufficient temporal and spatial resolution for kinematic analysis.

With respect to the door mechanism, one requirement was to avoid stress and prevent aversion to the entrance. To address this, a passive door was implemented, allowing animals to cross freely under their own volition by pushing the door. Another requirement was the need for individual identification to assign behavioural metrics to the correct subject. This was fulfilled by the use of RFID sensors. Finally, it was necessary to prevent multiple animals from accessing the reaching chamber simultaneously and interfering with one another during the task. This requirement was met through the stopper system, which physically regulates entry and guarantees that only one animal can perform the task at a time.

5.2 Experimental guidelines

This section details the guidelines required to reproduce both the RtG task and the process of transitioning animals between the home-cage and a task module.

Given that the paradigm employed throughout this work was the RtG task, the corresponding behavioural metrics will be used here as reference standards. Nevertheless, the structure of the protocol is designed to be adaptable, allowing for modifications according to the specific objectives of potential studies.

For the purposes of these guidelines, it is assumed that the final configurations of the reaching chamber (Version 0.5) and the door mechanism (Version 1.1) are being used.

5.2.1 Reach-to-grasp task

To habituate animals to perform the RtG task for water, it is necessary to ensure adequate motivation. Animals should be placed under a controlled water-restriction regime while following standard welfare guidelines. Prior to the first training session, water can be withheld for approximately 24 hours to ensure initial engagement with the task. Following this, water should be provided in measured amounts, ensuring each animal consumes at least 1 ml per day to maintain mild motivation while preventing dehydration or undue stress.

Begin with an initial habituation phase where animals explore the reaching chamber freely to promote familiarity with the setup. Position the water spout as close as possible to the slit aperture, ideally at a lickable distance, so that animals can easily detect the reward. If necessary, a small droplet of water can be left directly on the slit to attract attention and encourage initial licking. Once animals engage reliably, gradually displace the spout outward to progressively increase the reaching distance. Advancement through this shaping process should be guided by performance criteria, such as a minimum success rate, before further increasing the distance.

To promote consistent use of a specific forelimb, position the water spout horizontally opposite to the desired paw. For example, to enforce right forelimb use, displace the spout toward the left side of the slit. An offset of 5 mm from the slit centre is suggested for a slit width of 9.5 mm, but this value can be adjusted depending on observed behaviour to ensure reliable performance with the correct forelimb.

Conduct sessions in a quiet environment free from disturbances, keep session durations within reasonable limits to prevent fatigue and to ensure that the animals associate the sessions with a time when they should perform the RtG task. Adjustments should be made if necessary to maintain well-being while shaping reliable task performance.

5.2.2 Transition between compartments

To habituate animals to transition between the home-cage and an external task module, it is recommended to begin with an open tunnel that allows free exploration of both compartments. During this phase, animals can familiarise themselves with the tunnel environment without constraints. Since in this case, animals are under water restriction, their natural motivation facilitates exploration; however, if they show little initiative to cross spontaneously, small droplets of water may be placed along the tunnel to further encourage passage.

When training multiple animals, it is advisable to begin with individual sessions until each subject reliably performs the task, in this case the RtG movement. Only once animals are comfortable crossing

the tunnel in both directions and performing the task should they be grouped together. At this stage, continued monitoring is required to ensure that no animal develops a strong aversion or ceases to cross.

In this specific case, animals typically can reach adequately within the first one or two sessions. This rapid acquisition eliminates the need for a separate pre-training phase dedicated exclusively to the RtG task as both crossing and task performance can be shaped simultaneously.

Following this initial habituation, the open tunnel is replaced by a passive door system so that mice can learn to push the door to access the chamber. Our results suggest that a single session with a passive door is enough. Finally, to regulate mice's access, ensuring that only one animal enters the task module at a time the RFID-controlled door stopper system is introduced.

Accurate identification of individuals must also be guaranteed, for which RFID-based recognition is recommended.

Conduct sessions in a quiet environment free from disturbances. Although the setup enables 24/7 operation, animals need to be weighted and checked daily to ensure adequate welfare.

Chapter 6

Discussion and Final Conclusions

This work set out to develop a high-throughput setup for the automated measurement of skilled motor control in mice, providing a framework that can support long-term, minimally supervised behavioural experiments. The primary goal was technological: to design and validate a system capable of recording fine forelimb movements with high temporal precision while enabling continuous operation in a home-cage environment. Such a platform responds to a growing need in behavioural neuroscience for methods that combine experimental rigour with the scalability required for longitudinal studies of motor learning and adaptation.

To achieve this, we chose the RtG paradigm as the reference behavioural task. This well-established assay reliably elicits skilled, repeatable forelimb movements, making it an ideal benchmark for testing both the hardware and the analytical pipeline of a high-throughput system. Its demands on precision, kinematic resolution, and repetition allowed us to stress-test the setup and confirm that it could capture subtle motor features across extended timescales.

While the setup is agnostic to specific disease models, its design naturally lends itself to translational applications. As a proof of principle, we applied the system to experiments involving mice carrying the DYT-TOR1A mutation with the aim of modelling task-specific dystonia, a disorder linked to repetitive and dexterous motor actions [45], [47]. This case study illustrates how the setup can be adapted to investigate a broad range of questions, from normal motor learning to the progression of movement disorders.

The first stage focused on the creation of a reaching chamber, so that the RtG task itself would be as automated and stable as possible before connecting this module to the home-cage. For the basic hardware design, we took inspiration from the setup described by Galiñanes *et al.* [10], and then introduced a series of modifications to meet the specific requirements of our application.

To troubleshoot the problems encountered and to validate the setup, two experimental procedures (described in Section 3.3.1 and 3.3.2) were carried out, from which several important conclusions emerged. We found that we could impose the use of a specific forelimb by adjusting the position of both the slit and the water droplet. Additionally, we decided to employ a mirror instead of an additional camera to obtain a frontal view of the task, which made the setup considerably more economical.

Moreover, it is crucial that the setup remains consistent throughout all sessions, which requires that lighting conditions and the positioning of every component remain as reliable as possible. To achieve this, we used an infra-red spotlight and mounted all components on a Thorlabs breadboard.

Regarding the software, protocols were implemented to automate water delivery, video capture and data logging, ensuring that all these metrics could be reliably saved while minimising the need for experimenter intervention. The video capture protocol, described in Section 3.1.2.4, was particularly important

since the setup is intended for future use in a 24/7 regime, making continuous recording unfeasible. This protocol enabled the creation of short clips, optimising data storage while ensuring that all reaching movements were recorded.

The second stage of this work focused on analysing these clips. To achieve this, a motion-tracking pipeline was developed to study forelimb movement. We began by tracking several keypoints in the videos using DLC, obtaining highly reliable results that confirmed the quality of the recordings. From the coordinates of these keypoints, an analysis pipeline was created to ensure that the DLC outputs were robust and could be transformed into meaningful insights.

In this exploratory analysis, we examined the trajectory, velocity and acceleration profiles of the reaching movement, as well as derived multiple metrics from these data. Although the experiments analysed were preliminary and conducted in individual sessions, we were able to extract several interesting findings (Figure 4.8). For instance, we observed that WT animals displayed a decreasing trend in initial direction error across weeks, whereas DYT animals remained stable. This parameter will be important to monitor in future experiments performed in a 24/7 setting.

Beyond the kinematic analysis, EMG and in vivo calcium imaging recordings were also carried out during the pilot experiment, allowing us to confirm the feasibility of this individual setup for wired recordings (Figures 4.9 and 4.10). In future work, these approaches could be valuable for correlating such measurements with kinematic features.

While group comparisons across weeks can yield useful insights, the RtG task is inherently variable. Individual mice frequently adopt different motor strategies to execute the movement, so apparent group-level differences may reflect natural variation between animals rather than consistent adaptive changes. This highlights the need for larger sample sizes and more controlled conditions to disentangle true motor adaptations from noise in behavioural performance.

Following the analysis, the final stage of this work was to adapt the reaching chamber and connect it to the animal's home-cage so that the task could be performed in a 24/7 setting. To achieve this, it was necessary to design a door mechanism capable of both individualising and correctly identifying the animals as they moved between compartments.

After several iterations and tests, a system was developed that combined an RFID sensor with a stopper mechanism, enabling animals to cross from one side to the other without difficulty. The system employs a passive door that the animals can push open themselves, avoiding stress or interference with the task while still allowing reliable individual identification.

During these iterations, it became clear that not all engineering goals could be achieved without adaptation. The active servo-driven door (Version 1.0), although technically feasible, generated auditory and mechanical cues that the mice found aversive when its operation was not under their direct control. This led to avoidance behaviour and reduced voluntary task engagement. In contrast, the stopper system with a passive door (Version 1.1), although technically simpler, successfully prevented multiple entries and maintained high task engagement, demonstrating that a mechanism which appears optimal from a purely mechanical perspective may fail if it disrupts the animal's naturalistic sense of control and predictability.

In the end, we achieved a setup designed for high repeatability, automation and minimal experimenter intervention, allowing for the systematic study of motor function and dysfunction in mice. This setup enables automated acquisition of behavioural data under tightly controlled and reproducible conditions, making it a robust tool for investigating several hypotheses, in this case both the emergence and progression of dystonia-related motor abnormalities.

The modular structure of the setup also allows for easy and rapid optimisation. In the future, we

suggest the implementation of additional components such as weight or pressure-sensitive thresholds on the turnstile, adapted to mouse body mass, to unlock the stopper system. Furthermore, although a refill system has already been established, it could be improved by incorporating a bubble sensor in the fluidic line to detect air and prevent false pump counts.

In conclusion, this work establishes a flexible, high-throughput setup capable of supporting longitudinal studies of motor learning, adaptation, and pathology in mice. By bridging the gap between highly controlled experimental tasks and naturalistic behaviour, our system provides a unique opportunity to investigate not only task-specific dystonia but also a broader range of motor disorders and neurophysiological hypotheses. Its 24/7 automation, modular design, and reliable individual identification make it generalisable and suitable for diverse experimental paradigms.

By enabling continuous, minimally invasive monitoring of skilled forelimb movements, the setup lays the foundation for next-generation studies that combine hypothesis-driven and exploratory approaches. This capability supports translational neuroscience by allowing systematic, longitudinal assessment of motor function, adaptation, and dysfunction in mice, ultimately advancing our understanding of the mechanisms underlying both normal and pathological motor behaviours.

Bibliography

[1] G. Jansson and G. Johansson, "Visual perception of bending motion", *Perception*, vol. 2, no. 3, pp. 321–326, 1973.

[2] A. Mathis et al., "Deeplabcut: Markerless pose estimation of user-defined body parts with deep learning", *Nature neuroscience*, vol. 21, no. 9, pp. 1281–1289, 2018.

[3] X. Wu, D. Sahoo, and S. C. H. Hoi, *Recent advances in deep learning for object detection*, 2019.

[4] D. H. O'Connor, D. Huber, and K. Svoboda, "Reverse engineering the mouse brain", *Nature*, vol. 461, no. 7266, pp. 923–929, 2009.

[5] L. Berg, J. Gerdey, and O. A. Masseck, "Optogenetic manipulation of neuronal activity to modulate behavior in freely moving mice", *J Vis Exp*, vol. 164, no. 10.3791, p. 61 023, 2020.

[6] L.-A. R. Sacrey, M. Alaverdashvili, and I. Q. Whishaw, "Similar hand shaping in reaching-for-food (skilled reaching) in rats and humans provides evidence of homology in release, collection, and manipulation movements", *Behavioural brain research*, vol. 204, no. 1, pp. 153–161, 2009.

[7] E. C. Bryda, "The mighty mouse: The impact of rodents on advances in biomedical research", *Missouri medicine*, vol. 110, no. 3, p. 207, 2013.

[8] A. Domínguez-Oliva, I. Hernández-Ávalos, J. Martínez-Burnes, A. Olmos-Hernández, A. Verduzco-Mendoza, and D. Mota-Rojas, "The importance of animal models in biomedical research: Current insights and applications", *Animals*, vol. 13, no. 7, p. 1223, 2023.

[9] A. Bova, M. Gaidica, A. Hurst, Y. Iwai, J. Hunter, and D. K. Leventhal, "Precisely timed dopamine signals establish distinct kinematic representations of skilled movements", *Elife*, vol. 9, e61591, 2020.

[10] G. L. Galiñanes, C. Bonardi, and D. Huber, "Directional reaching for water as a cortex-dependent behavioral framework for mice", *Cell reports*, vol. 22, no. 10, pp. 2767–2783, 2018.

[11] G. Salameh, M. S. Jeffers, J. Wu, J. Pitney, and G. Silasi, "The home-cage automated skilled reaching apparatus (hasra): Individualized training of group-housed mice in a single pellet reaching task", *eneuro*, vol. 7, no. 5, 2020.

[12] C. T. Miller et al., "Natural behavior is the language of the brain", *Current Biology*, vol. 32, no. 10, R482–R493, 2022.

[13] M. J. Beetz, "A perspective on neuroethology: What the past teaches us about the future of neuroethology", *Journal of Comparative Physiology A*, vol. 210, no. 2, pp. 325–346, 2024.

[14] H. H.-W. Wong, C. Y. C. Chou, A. J. Watt, and P. J. Sjöström, "Comparing mouse and human brains", *Elife*, vol. 12, e90017, 2023.

[15] T. E. Bakken et al., "Comparative cellular analysis of motor cortex in human, marmoset and mouse", *Nature*, vol. 598, no. 7879, pp. 111–119, 2021.

[16] J. M. Hickman-Davis and I. C. Davis, "Transgenic mice", *Paediatric respiratory reviews*, vol. 7, no. 1, pp. 49–53, 2006.

[17] M. A. Rossi and H. H. Yin, "Methods for studying habitual behavior in mice", *Current protocols in neuroscience*, vol. 60, no. 1, pp. 8–29, 2012.

[18] D. L. Schacter, D. T. Gilbert, D. M. Wegner, and M. Nock, "Bf skinner: The role of reinforcement and punishment", *Psychology*, pp. 278–288, 2011.

[19] J. R. Krebs, "Animal behaviour: From skinner box to the field", *Nature*, vol. 304, no. 5922, pp. 117–117, 1983.

[20] A. Silva, P. Carriço, A. B. Fernandes, T. Saraiva, A. J. Oliveira-Maia, and J. A. da Silva, "High-precision optical fiber-based lickometer", *eneuro*, vol. 11, no. 7, 2024.

[21] S. N. Katner, J. G. Magalong, and F. Weiss, "Reinstatement of alcohol-seeking behavior by drug-associated discriminative stimuli after prolonged extinction in the rat", *Neuropsychopharmacology*, vol. 20, no. 5, pp. 471–479, 1999.

[22] N. Hymowitz, "Effects of lever-press-dependent and independent electric shock on schedule-induced water intake", *The Psychological Record*, vol. 23, no. 4, pp. 487–497, 1973.

[23] J. Wilkenfield, M. Nickel, E. Blakely, and A. Poling, "Acquisition of lever-press responding in rats with delayed reinforcement: A comparison of three procedures", *Journal of the Experimental analysis of behavior*, vol. 58, no. 3, pp. 431–443, 1992.

[24] C. A. Bruner, A. S. Raul, L. Acuña, and L. M. Gallardo, "Effects of reinforcement rate and delay on the acquisition of lever pressing by rats", *Journal of the Experimental analysis of behavior*, vol. 69, no. 1, pp. 59–75, 1998.

[25] A. Klein, L.-A. R. Sacrey, I. Q. Whishaw, and S. B. Dunnett, "The use of rodent skilled reaching as a translational model for investigating brain damage and disease", *Neuroscience & Biobehavioral Reviews*, vol. 36, no. 3, pp. 1030–1042, 2012.

[26] D. J. Ellens et al., "An automated rat single pellet reaching system with high-speed video capture", *Journal of Neuroscience Methods*, vol. 271, pp. 119–127, 2016.

[27] M. J. Wagner, J. Savall, T. H. Kim, M. J. Schnitzer, and L. Luo, "Skilled reaching tasks for head-fixed mice using a robotic manipulandum", *Nature protocols*, vol. 15, no. 3, pp. 1237–1254, 2020.

[28] M. S. Esposito, P. Capelli, and S. Arber, "Brainstem nucleus mdv mediates skilled forelimb motor tasks", *Nature*, vol. 508, no. 7496, pp. 351–356, 2014.

[29] J.-Z. Guo et al., "Cortex commands the performance of skilled movement", *Elife*, vol. 4, e10774, 2015.

[30] X. Wang et al., "Deconstruction of corticospinal circuits for goal-directed motor skills", *Cell*, vol. 171, no. 2, pp. 440–455, 2017.

[31] E. A. de Laittre and J. N. MacLean, "The natural variability of a dexterous motor skill is stably encoded in the cortex of freely behaving mice", *bioRxiv*, pp. 2024–12, 2024.

[32] I. Q. Whishaw et al., "Organization of the reach and grasp in head-fixed vs freely-moving mice provides support for multiple motor channel theory of neocortical organization", *Experimental brain research*, vol. 235, pp. 1919–1932, 2017.

[33] G. Lopes et al., "Bonsai: An event-based framework for processing and controlling data streams", *Frontiers in neuroinformatics*, vol. 9, p. 7, 2015.

[34] A. Gomez-Marin, J. J. Paton, A. R. Kampff, R. M. Costa, and Z. F. Mainen, "Big behavioral data: Psychology, ethology and the foundations of neuroscience", *Nature neuroscience*, vol. 17, no. 11, pp. 1455–1462, 2014.

[35] D. J. Anderson and P. Perona, "Toward a science of computational ethology", *Neuron*, vol. 84, no. 1, pp. 18–31, 2014.

[36] A. I. Dell et al., "Automated image-based tracking and its application in ecology", *Trends in ecology & evolution*, vol. 29, no. 7, pp. 417–428, 2014.

[37] T. Nath, A. Mathis, A. C. Chen, A. Patel, M. Bethge, and M. W. Mathis, "Using deeplabcut for 3d markerless pose estimation across species and behaviors", *Nature protocols*, vol. 14, no. 7, pp. 2152–2176, 2019.

[38] T. D. Pereira et al., "Sleap: A deep learning system for multi-animal pose tracking", *Nature methods*, vol. 19, no. 4, pp. 486–495, 2022.

[39] J. Lauer et al., "Multi-animal pose estimation, identification and tracking with deeplabcut", *Nature Methods*, vol. 19, no. 4, pp. 496–504, 2022.

[40] K. Wangi and A. Makandar, "Cnn pre-trained model using the fusion of features for cbir framework", in *2024 International Conference on Recent Advances in Electrical, Electronics, Ubiquitous Communication, and Computational Intelligence (RAEEUCCI)*, IEEE, 2024, pp. 1–5.

[41] P. Karashchuk et al., "Anipose: A toolkit for robust markerless 3d pose estimation", *Cell reports*, vol. 36, no. 13, 2021.

[42] J. Armshaw, G. Butcher, and A. Becker, "Gathering self-initiated rat behavioral data to characterize post-stroke deficits", *Journal of Visualized Experiments (JoVE)*, no. 205, e64967, 2024.

[43] G. Butcher, A. Davidson, A. Sloan, L. Schneider, A. Lund, and A. Becker, "An apparatus for automatically training and collecting individualized behavioral data with socially housed rodents", *Journal of Neuroscience Methods*, vol. 365, p. 109 387, 2022.

[44] A. Albanese et al., "Definition and classification of dystonia", *Movement Disorders*, 2025.

[45] E. Altenmüller and H.-C. Jabusch, "Focal dystonia in musicians: Phenomenology, pathophysiology and triggering factors", *European Journal of Neurology*, vol. 17, pp. 31–36, 2010.

[46] A. L. McKenzie, S. Goldman, C. Barrango, M. Shrime, T. Wong, and N. Byl, "Differences in physical characteristics and response to rehabilitation for patients with hand dystonia: Musicians' cramp compared to writers' cramp", *Journal of Hand Therapy*, vol. 22, no. 2, pp. 172–182, 2009.

[47] V. E. Rozanski, E. Rehfuess, K. Bötzel, and D. Nowak, "Task-specific dystonia in professional musicians: A systematic review of the importance of intensive playing as a risk factor", *Deutsches Aerzteblatt International*, vol. 112, no. 51-52, p. 871, 2015.

[48] B. György et al., "Mutant torsina in the heterozygous dyt1 state compromises hsv propagation in infected neurons and fibroblasts", *Scientific reports*, vol. 8, no. 1, p. 2324, 2018.

[49] C. Reinhold et al., "Gene-environment interaction elicits dystonia-like features and impaired translational regulation in a dyt-tor1a mouse model", *Neurobiology of Disease*, vol. 193, p. 106 453, 2024.

[50] B. F. Cruz et al., "A flexible fluid delivery system for rodent behavior experiments", *bioRxiv*, pp. 2024–04, 2024.

[51] E. Insafutdinov, L. Pishchulin, B. Andres, M. Andriluka, and B. Schiele, "Deepercut: A deeper, stronger, and faster multi-person pose estimation model", in *Computer Vision–ECCV 2016: 14th European Conference, Amsterdam, The Netherlands, October 11-14, 2016, Proceedings, Part VI 14*, Springer, 2016, pp. 34–50.

[52] K. He, X. Zhang, S. Ren, and J. Sun, "Deep residual learning for image recognition", in *Proceedings of the IEEE conference on computer vision and pattern recognition*, 2016, pp. 770–778.

[53] A. E. Urai, V. Aguillon-Rodriguez, I. C. Laranjeira, F. Cazettes, Z. F. Mainen, A. K. Churchland, et al., "Citric acid water as an alternative to water restriction for high-yield mouse behavior", *Eneuro*, vol. 8, no. 1, 2021.

[54] B. Chung et al., "Myomatrix arrays for high-definition muscle recording", *Elife*, vol. 12, RP88551, 2023.

[55] M. D. Mendonca, J. A. da Silva, L. F. Hernandez, I. Castela, J. Obeso, and R. M. Costa, "Dopamine neuron activity encodes the length of upcoming contralateral movement sequences", *Current Biology*, vol. 34, no. 5, pp. 1034–1047, 2024.

[56] M. A. Zolotykh and E. N. Kozhevnikova, "The effect of social experience on olfactory preference in male mice", *Applied Animal Behaviour Science*, vol. 189, pp. 85–90, 2017.

Chapter 7

Appendix

7.1 Appendix A

This section presents the abstract and poster selected for presentation at XIX Meeting of the Portuguese Society of Neuroscience, held in Póvoa de Varzim, Portugal, from 28 to 30 May 2025, titled "A High-Throughput 24/7 Reach-to-Grasp System for Investigating Motor Control and Movement Disorders".

A High-Throughput 24/7 Reach-to-Grasp System for Investigating Motor Control and Movement Disorders

M.V. Bettencourt[1], **A. Germano**[1,2], F. França de Barros[1,3], J. Alves da Silva[1,3]

[1]Champalimaud Research, Champalimaud Foundation, Portugal
[2]Faculdade de Ciências da Universidade de Lisboa, Portugal
[3]NOVA Medical School, Faculdade de Ciências Médicas, Universidade Nova de Lisboa, Portugal

Dystonia is a movement disorder characterised by involuntary muscle contractions leading to abnormal postures or movements. When extensively performed, dexterous motor activities, such as writing or playing an instrument, can lead to a particular type of dystonia known as task-specific dystonia. In this type of dystonia, involuntary muscle contractions happen specifically when performing such actions. Nevertheless, the neural circuit dysfunctions underpinning this disease remain unclear. Having an adequate animal model of task-specific dystonia is an essential step to detail the pathophysiology of this disease. However, current animal studies relying on the execution of repetitive actions have had limited success in replicating a phenotype of task-specific dystonia. Insufficient trial numbers and reproducibility have been identified as potential constraints in previous approaches.

To address these limitations, we are developing a fully automated 24/7 reach-to-grasp (RtG) training system that integrates seamlessly into a home-cage environment, allowing continuous and individualised, ad libitum high-repetition training in group-housed mice. This task offers a predictable motor output and precise movement characterisation while enabling the comparison of movement patterns in a controlled, freely-moving environment. By allowing training throughout the whole day, we are maximizing the number of repetitions of a skilled movement, a preponderant factor for the development of task-specific dystonia.

7. APPENDIX

Our setup consists of a training chamber, connected to a standard home-cage via a rotating door, with an adjustable reaching module that delivers water drops through a servo-controlled needle. This system enforces lateralized forelimb reaching while leveraging an RFID-based identification system to track individual mice. High-speed cameras and an orthogonal mirror setup enable video-based 3D kinematic tracking of reaching movements without the need for external markers or invasive sensors. An automated detection algorithm ensures real-time water delivery and video acquisition of relevant trials, optimizing storage and analysis.

Preliminary validation in a prototype system has demonstrated scalability and reproducibility. Early data indicate that mice rapidly learn the task, and stepwise modifications to water drop distance successfully modulate training intensity. Furthermore, changing the position of the water drop can also be used to force mice to use a specific forelimb. These findings confirm the feasibility of our approach and highlight its potential for high-throughput behavioural assessments in movement disorder research.

Combining this automated 24/7 RtG system with dystonia-related transgenic mouse lines will provide an unprecedented opportunity to develop a high-validity task-specific dystonia animal model, fundamental for understanding the pathophysiology of this debilitating disease.

A high-throughput reach-to-grasp system for investigating motor control and movement disorders

M.V. Bettencourt[1], A. Germano[1,2], F. França de Barros[1,3], J. Alves da Silva[1,3]

[1]Champalimaud Research, Champalimaud Foundation, Lisboa, Portugal ; [2]Faculdade de Ciências da Universidade de Lisboa, Lisboa, Portugal ; [3]NOVA Medical School, Faculdade de Ciências Médicas, Universidade NOVA de Lisboa, Lisboa, Portugal.

Introduction

Studying skilled forelimb movements in rodents is essential for understanding motor control and its dysfunctions. However, current reach-to-grasp paradigms are often limited by **low trial throughput, manual supervision, and poor adaptability to naturalistic settings.**

These constraints hinder the scalability, reproducibility, and translational relevance of behavioural studies in mouse models.

Aims & Methods

Build an automatized and autonomous 24/7 high-throughput reach-to-grasp setup for mice

We combined automated water-based training, video acquisition, and markerless motion tracking techniques to enable continuous high-resolution assessment of forelimb kinematics.

A **dystonia** (DYT) mouse model was used to showcase the applicability of the setup for monitoring motor impairments induced by repetitive dexterous movements.

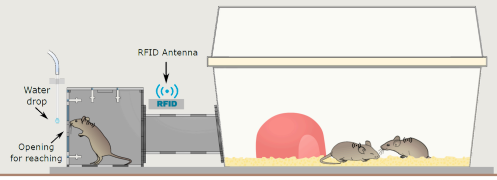

Results

Reach-to-Grasp Pilot Experiment

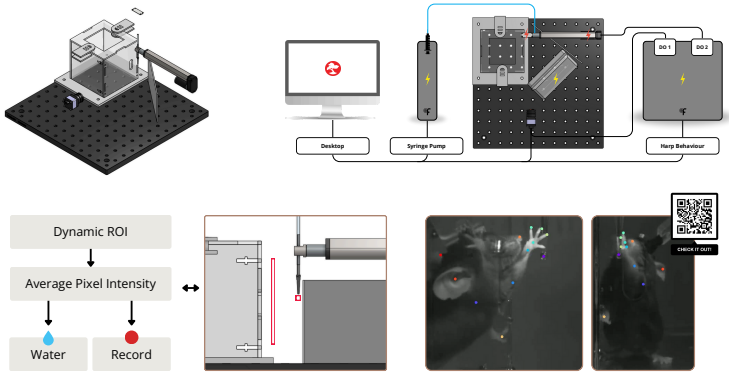

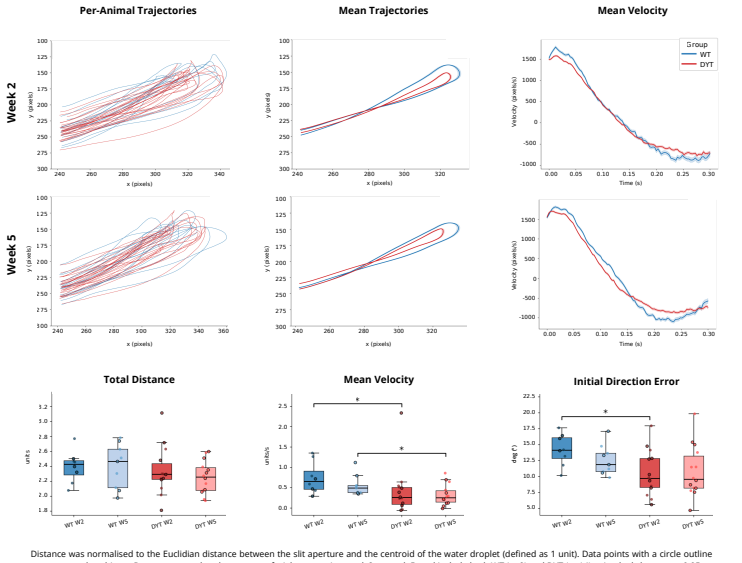

Distance was normalised to the Euclidian distance between the slit aperture and the centroid of the water droplet (defined as 1 unit). Data points with a circle outline represent male subjects. Data correspond to the average of trials comparing week 2 vs week 5, and include both WT (n=9) and DYT (n=14) animals. * denotes p<0.05.

Towards Full 24/7 Automatization

To transition the setup to a fully **24/7 operation**, we need to ensure:
Individualised & identifiable access Autonomous water refill

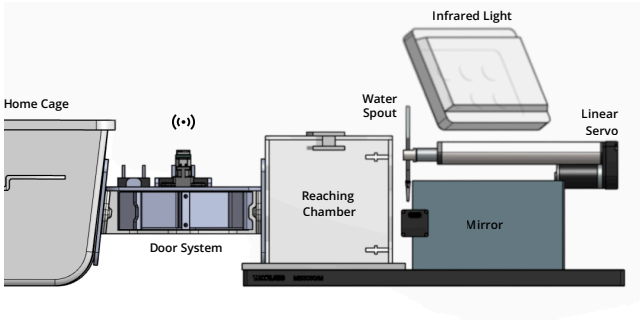

RFID Controlled Door System

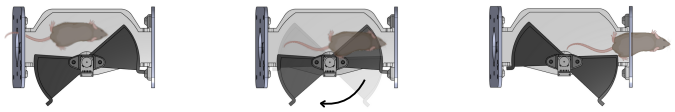

Each mouse is identified when passing through the central **RFID sensor**, a mechanism that functions identically in both directions, allowing accurate logging of entries and exits.

Pump Refill System

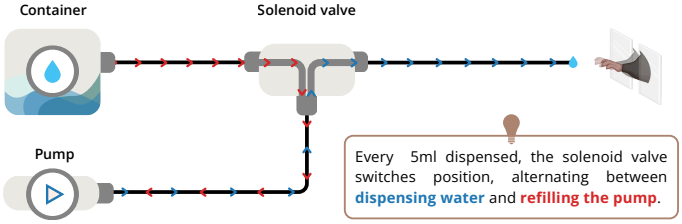

Every 5ml dispensed, the solenoid valve switches position, alternating between **dispensing water** and **refilling the pump**.

Conclusion

We established the fundamental steps to develop a scalable, automated reach-to-grasp setup capable of continuous behavioural tracking in mice. The system enables high-throughput kinematic analysis with **minimal human intervention**, highlighting its potential for **studying motor impairments** in naturalistic conditions, pivotal for understanding movement disorders.

Future Work

The current RFID-based door access control is still under testing; therefore, future efforts are focused on **improving robustness and reliability** to ensure **seamless 24/7 operation** in group-housed conditions.

Ackowledgements
Artur Silva[1], Hugo Marques[1], José Grilo[1], Joseph Tutt[1], Nuno Matela[2], Pedro Dias[1] and Simon Zamora[1]

Supported by
Dystonia Medical Research Foundation

7.2 Appendix B

This section presents the abstract selected for oral presentation (top 3 best abstracts) at IMED Innovate Competition 17.0, held in Lisbon, Portugal, on 3 October 2025, titled "A High-Throughput 24/7 Reach-to-Grasp System for Investigating Motor Control and Movement Disorders".

A High-Throughput 24/7 Reach-to-Grasp System for Investigating Motor Control and Movement Disorders

A. Germano[1,2], J. Alves da Silva[1,3]

[1]Champalimaud Research, Champalimaud Foundation, Portugal
[2]Faculdade de Ciências da Universidade de Lisboa, Portugal
[3]NOVA Medical School, Faculdade de Ciências Médicas, Universidade Nova de Lisboa, Portugal

Introduction

Current approaches to study motor control in rodents are constrained by low trial throughput, manual intervention, and limited ecological validity. These limitations are particularly evident in the context of task-specific motor disorders (such as task-specific dystonia), where high-frequency, longitudinal behavioural data assessment is essential. To overcome these challenges, we aim to develop an automated, high-throughput reach-to-grasp (RtG) training system designed for 24/7 operation in group-housed mice. Our platform integrates real-time monitoring and individualised access to support continuous, goal-directed forelimb training with minimal experimenter involvement.

Methods

The training platform consists of a custom-designed behavioural chamber connected to the home-cage via an automated rotating door. Access is individually regulated using RFID identification, allowing mice to self-initiate experimental sessions without human supervision. Inside the chamber, mice access a lateralised water spout through a narrow slit, requiring a RtG movement to obtain approximately 5 μL of water per trial. The spout is mounted on a servo motor and can be repositioned across sessions to adjust task difficulty dynamically. Using a single high-speed camera and a 45º angled mirror, we obtain synchronised orthogonal (frontal and lateral) perspectives of each trial for kinematic analysis with DeepLabCut. As part of the validation phase, we implemented a semi-automated version of the system to test real-time behaviour detection and control logic using Bonsai RX. Additionally, we conducted two parallel experimental groups using mice implanted with intramuscular EMG electrodes and one-photon calcium imaging, respectively, aimed at evaluating the feasibility of combining kinematic analysis with physiological recordings to better understand motor control.

Results

Preliminary results indicate that mice rapidly learned the reaching task and performed approximately 200 trials in 30-minute sessions, a substantial increase compared to traditional food-pellet protocols. Kinematic features such as reach velocity, path efficiency, and movement smoothness were extracted. Real-time task control and synchronisation with behavioural markers were successfully achieved. EMG

and calcium imaging results confirmed that the system supports multimodal physiological integration without substantially altering behaviour.

Discussion

Unlike conventional setups limited by human supervision and trial scarcity, our system enables automated, high-resolution behavioural monitoring at scale. The modular design supports future integration of additional sensors and actuators, allowing closed-loop experiments and adaptive training protocols. While originally motivated by the need to model task-specific dystonia, the platform is broadly applicable to a range of questions in motor control and rehabilitation. The transition toward full 24/7 access will further enhance ecological validity and reproducibility.

Conclusion

We present a semi-automated RtG system capable of delivering high-frequency, goal-directed forelimb training in mice, with integrated behavioural and physiological monitoring. Current results support its scalability and potential for longitudinal motor assessments. As we transition toward full automation and continuous home-cage integration, this platform lays the foundation for next-generation studies of motor behaviour by combining high-throughput data collection with minimal experimenter interference, supporting both hypothesis-driven and exploratory neuroscience research.

7.3 Appendix C

Figure 7.1 (in the next page) presents the technical drawing of the main components of the door mechanism (Version 1.1). The connector pieces (with the dimensions shown in C) are designed to interface precisely with the support pieces (B) and the top acrylic cover. To ensure a proper fit, their length is reduced by 0.1 mm relative to the corresponding slots.

Note: This drawing is provided for information only and not for manufacturing purposes.

7.4 Appendix D

The observations of the reach adaptability test for the four animals are summarised below. The tip of the spout was moved approximately 2 mm closer for all animals.

M5316 experienced an upward spout adjustment of 7 mm. The animal reached the target easily, requiring only minor adjustments from previously trained movements.

M5318 had the spout raised by 10 mm. The animal achieved the higher position with slightly more stretching, showing some difficulty but performing effectively.

M5256 had the spout lowered by 10 mm. The animal initially reached straight and then downward. Adaptation required some effort, but movements were smooth, and with repeated exposure the task became easier, although slightly less natural due to prior training.

M5257 experienced a downward adjustment of approximately 15 mm. This position was initially challenging, and the animal needed to readjust its movements repeatedly. With practice, however, the animal adapted successfully.

7. APPENDIX

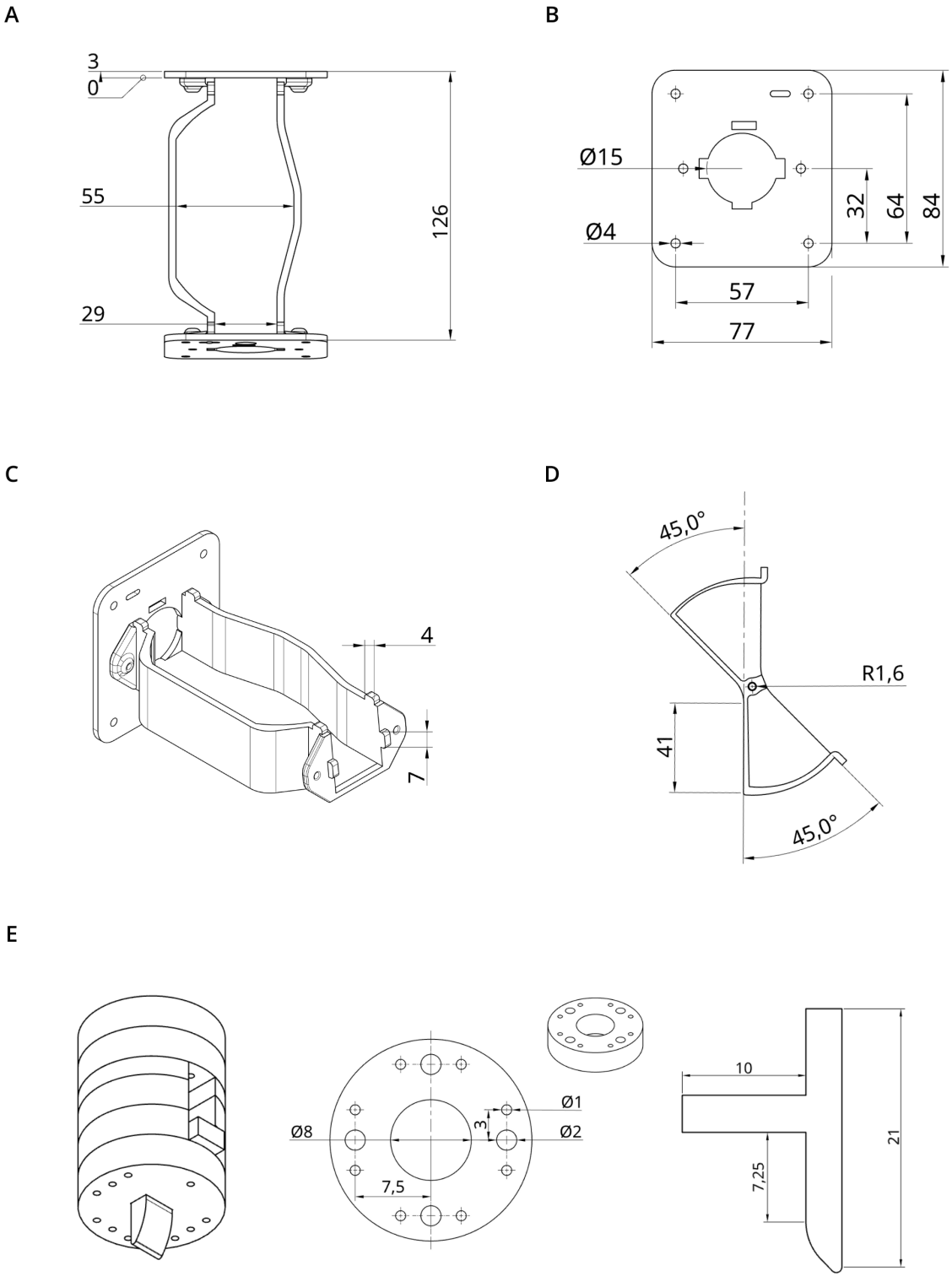

Figure 7.1: Technical drawing of the door mechanism components - Version 1.1. A – Top view of the base. B – Front view of a support piece. C – Isometric view of the base and a support piece with connector piece dimensions. D – Top view of the door. E – Stopper piece used in the door mechanism; the holes were designed to fit into the servo motor adapter. All dimensions are in millimetres and drawn to scale.

7.5 Appendix E

The final distances (and means) for each animal used in the pilot experiment are shown in the following tables:

Table 7.1: Final distances of each animal used in the pilot experiment.

Mouse ID	Sex	Genotype	Actuator Position	Distance (mm)
5176	♀	DYT	1650	15
5177	♀	DYT	1650	15
5212	♀	WT	1700	13
5242	♂	DYT	1600	17
5256	♀	DYT	1700	13
5257	♀	WT	1700	13
5266	♂	DYT	1650	15
5267	♂	DYT	1700	13
5278	♂	DYT	1650	15
5280	♂	DYT	1650	15
5281	♂	WT	1600	17
5282	♂	WT	1600	17
5283	♀	DYT	1650	15
5287	♀	WT	1700	13
5291	♀	WT	1550	19
5296	♂	DYT	1700	13
5316	♀	DYT	1650	15
5318	♀	WT	1600	17
5319	♀	DYT	1700	13
5327	♂	WT	1600	17
5329	♂	DYT	1600	17
5330	♀	DYT	1600	17
5334	♂	WT	1750	11
5335	♂	WT	1700	13

Note. WT – wild-type; DYT – heterozygous carrier of the DYT1 mutation; ♂ – Male; ♀ – Female. Distance in millimetres (mm). Each 50-step increment in actuator position corresponds to a 2 mm change in distance.

Table 7.2: Mean distance (mm) by genotype and sex, including marginal means.

Genotype / Sex	Female	Male	Genotype Mean
DYT	14.71	15.00	14.86
WT	15.00	15.00	15.00
Sex Mean	14.83	15.00	—